Energy Conversion and Management 195 (2019) 313–327

Contents lists available at ScienceDirect

Energy Conversion and Management

journal homepage: www.elsevier.com/locate/enconman

Conventional and energy level based exergoeconomic analysis of biomass and natural gas fired polygeneration system integrated with ground source heat pump and PEM electrolyzer

Xiaofeng Zhang[a,*], Rong Zeng[b], Tao Du[c], Yecong He[a], Hong Tian[a], Kang Mu[a], Xiaobo Liu[a], Hongqiang Li[d,*]

[a] College of Energy and Power Engineering, Key Laboratory of Efficient & Clean Energy Utilization, The Education Department of Hunan Province, Changsha University of Science and Technology, Changsha, Hunan 410114, China
[b] College of Civil Engineering and Mechanics, Xiangtan University, Xiangtan, Hunan 411105, China
[c] Faculty of Urban Construction and Environmental Engineering, Chongqing University, Chongqing 400045, China
[d] College of Civil Engineering, National Center for International Research Collaboration in Building Safety and Environment, Hunan University, Changsha, Hunan 410082, China

ARTICLE INFO

Keywords:
Exergoeconomic analysis
Energy level
Proton exchange membrane (PEM) electrolyzer
Geothermal energy
Hydrogen production

ABSTRACT

In this research, energy level based exergoeconomic evaluations are performed for a novel biomass and natural gas fired polygeneration system of electricity, hot water, chilled water and hydrogen production. The proposed system mainly consists of a biomass gasifier, a proton exchange membrane (PEM) electrolyzer, a gas turbine cycle (GT), an absorption chiller, and a ground source heat pump cycle. Conventional and energy level based exergoeconomic performances of the proposed system are compared; related exergy and economic analysis are also performed. In addition, the variations in unit exergy cost of products (electricity, hot water, chilled water and hydrogen) are studied under economic factors. The results show that energy and exergy efficiency of the electrolyzer and the proposed system decrease with the increasing current density of the PEM electrolyzer. The unit exergy cost of electricity and hydrogen are 5.24 $/GJ and 20.41 $/GJ under the energy level based exergoeconomic method, respectively, which are higher than that under the conventional exergoeconomic method (electricity: 4.38 $/GJ, hydrogen: 19.00 $/GJ), while the unit exergy cost of hot water and chilled water under the energy level based exergoeconomic method are lower than that under the conventional exergoeconomic method. Moreover, the exergoeconomic factor and relative cost difference of the system equipment also show distinctions under the conventional and energy level based exergoeconomic methods. The presented polygeneration system is a promising technology to utilize renewable energy and improve the flexibility of the integrated system; and the energy level based exergoeconomic method shows certain rationality and feasibility in the system analysis.

1. Introduction

Nowadays, renewable and clean energy are being utilized widely with the increasing energy consumption and limited reserves of fossil fuels. According to the report of International Energy Agency (IEA), renewable energy obtained the highest rate of growth of all energy resources in 2017, in which renewable energy based power generation accounts for about 25% of the world power generation [1]. Among all the renewable energies, the average annual growth rate of the geothermal energy is approximately 3.4% from 1990 to 2016, which is higher than the growth rate of the global total primary energy supply (1.7%) and the renewable energy sources (2%) [2]. As one of the promising clean energies, biomass accounts for approximately 14% of the global renewable energy utilization [3]. From 2012 to 2017, the installed capacity of biomass increased from 8 GW to 15 GW, and the power generation of biomass increased from 30 TWh to 79 TWh [4].

An energy generation system is crucial to energy efficiency and security of energy supply. The distributed energy system (DES) is attracting increasing attention due to low pollution emissions, energy saving and product diversity. It generally consists of combined cooling, heating and power (CCHP) system [5]; combined heating and power (CHP) system [6], and multi-generation (or poly-generation) system

* Corresponding authors.
E-mail addresses: xiaofengzhang@csust.edu.cn (X. Zhang), lhq@hnu.edu.cn (H. Li).

https://doi.org/10.1016/j.enconman.2019.05.017
Received 14 December 2018; Received in revised form 26 April 2019; Accepted 6 May 2019
Available online 11 May 2019
0196-8904/

Nomenclature

Abbreviation

CCHP	combined cooling, heating and power
CHP	combined heating and power
COP	coefficient of performance
DES	distributed energy system
ER	equivalence ratio
GCU	gas conditioning unit
GMR	gas mass ratio
GSHP	ground source heat pump
GT	gas turbine cycle
HHV	higher heating value
HX	heat exchanger
LHV	lower heating value
O&M	operation & maintenance
PEM	proton exchange membrane
SR	split ratio
ST	steam turbine cycle

Symbols

A	energy level
$\dot{C}$	cost rate ($/h)
CRF	capital recovery factor
c	unit exergy cost ($/GJ)
dE	exergy change (kJ)
dH or ΔH	enthalpy change (kJ)
dS or ΔS	entropy change (kJ/K)
E	electricity (kW)
E_{act}	activation energy (kJ/mol)
EX	exergy (kW)
ex	specific exergy (kJ/kg)
F	Faraday constant (C/mol)
f	exergoeconomic factor (%)
G	Gibbs free energy (kJ)
H	enthalpy (kJ)
J	current density (A/m^2)
J_0	exchange current density (A/m^2)
J^{ref}	pre-exponential factor (A/m^2)
L	membrane thickness (μm)
m	mass flow rate (kg/h)
N	molar flow rate (mol/s)
n	service life (year)
P	interest rate (%)
Q	heat (kW)
R	universal gas constant (kJ/kmol·K)
R_{PEM}	overall ohmic resistance (Ω)
S	square (m^2)
T	temperature (K)
V	voltage (V)
V_0	reversible potential (V)
$V_{act,a}$	activation overpotential of anode (V)
$V_{act,c}$	activation overpotential of cathode (V)
V_{con}	concentration overpotential (V)
V_{ohm}	ohmic overpotential (V)
W	power (kW)
$\dot{Z}$	investment cost rate ($/h)
σ	ionic conductivity (s/m)
λ	operation and maintenance cost ratio (%)
$\lambda(x)$	water content at location of x in membrane (Ω^{-1})
λ_a	water content at anode-membrane interface (Ω^{-1})
λ_c	water content at cathode-membrane interface (Ω^{-1})
γ_p	compressor ratio
τ	annual operating hour (h)
η	efficiency (%)

Subscripts

a	anode
AB	absorption chiller
AC	air compressor
C	cooling
c	cathode
CI	capital investment
COM	compressor
CON	condenser
D	destruction
ele	electricity
EVA	evaporator
f	fuel
G	gasifier
GC	bio-gas compressor
GM	gas mixer
GT	gas turbine
H	heating
is	isentropic
L	loss
OM	operation & maintenance investment
p	product
P	pump

[7]. In China, there are abundant biomass resources; the total amount of biomass resources for energy utilization is about 460 million tons of standard coal every year, especially for rice husk, because rice-planting, with rice being an important grain crop, is very popular in south China. The annual exploitable resources of shallow geothermal energy are equivalent to 700 million tons of standard coal according to «*the 13th Five Year Plan for Development and Utilization of Geothermal Energy*». Considering the abundant biomass and geothermal energy resources, it provides possibility for developing these two renewable based DESs. Besides that, the DES mainly provides users with heating, cooling and power considering the daily energy demands. In addition, to improve the flexibility of the energy generation system, the hydrogen production technology is an alternative by converting excess electricity to hydrogen. To further analyze the technical and economic feasibility of the proposed system, a suitable exergoeconomic analysis should be considered.

1.1. Biomass and geothermal based DES

Some researchers have studied some DESs based on the biomass or geothermal energy [8,9]. Habibollahzade et al. [8] presented an integrated system coupled with biomass gasification, a solid oxide fuel cell, a Stirling engine and an electrolyzer, which was optimized by the multi-objective optimization method. Ahmadi [10] performed thermodynamic performances of a biomass based multi-generation energy system with electricity, cooling, hydrogen, and hot water production. A parameter study was also considered to analyze the effects of key design variables on system performances. Bai et al. [11] proposed and modeled a power generation system based on biomass and solar energy, the results showed that the proposed two-stage solar-biomass model could improve the system thermodynamic performance and an overall energy efficiency of 27.93% could be achieved. Besides the biomass based energy systems, the geothermal based energy systems are also studied. Mohammadi and Mehrpooya [12] presented a novel system integrated with a geothermal flash, Kalina and Reverse osmosis system, and carried out sensitivity analysis based on the key thermodynamic parameters. Amirmohammad et al. [13] proposed a cogeneration system consisting of a geothermal plant, a photovoltaic/thermal system and a double-effect absorption chiller. The multi-objective optimization method was carried out to minimize the product unit cost and maximize the system exergy efficiency. He et al. [14] proposed a combined power and water system taking geothermal energy as co-feeds; the combined system was mainly composed of an organic Rankine cycle and a desalination system. System performances were investigated in terms of energy, entropy and cost aspects. For the biomass and geothermal energy coupling system, Malik et al. [15] proposed a biomass and geothermal based multi-generation system with five distinct products for residential applications. The energy and exergy efficiencies of the proposed multi-generation system increased by 44.7% and 2.9% compared with the single generation system. Srinivas et al. [16] compared and analyzed different configurations of a biomass combustor and the existing geothermal electricity plant from the perspectives of thermodynamics and economics, which contributed to increasing the electricity output of the turbine under a cost-effective condition.

In biomass gasification-based DES, the common power generation units (PGU) are: internal combustion engine, gas turbine and solid oxide fuel cell. From the perspectives of technology development and investment cost, internal combustion engine and gas turbine are the most common power generation units. Moreover, the emission of a gas turbine is relatively lower than that of internal combustion engine [17]. At the same time, ground source heat pump (GSHP) is one of the promising technologies for geothermal utilization. Therefore, this study considers integrating biomass gasification process, gas turbine cycle and GSHP. Zhang et al. [18] made an exergetic and exergoeconomic analysis of a CHP system taking biomass and geothermal energy as cofeeds, and optimized the capacity and operation strategy of proposed system in terms of energy, economic and environmental aspects [19]. Furthermore, the natural gas was introduced and the cooling load was also considered in the novel CCHP system so as to improve the reliability and provided more outputs [20], while this CCHP system didn't consider how to deal with surplus electricity.

1.2. Proton exchange membrane (PEM) electrolyzer based DES

As an alternative energy carrier hydrogen has many advantages, such as environment friendly, high energy density and safety [21,22]. There are many processes for hydrogen production such as the chemical process, biological process, electrolytic process, thermo-chemical process, etc. A variety of resources can be considered as raw materials, such as coal, natural gas, biomass, water, etc [23]. Among the hydrogen production technologies, water electrolysis is a mature technique for hydrogen generation at large scales. Proton exchange membrane (PEM) electrolysis has drawn increasing attention due to high voltage efficiency and environmental effects [24,25].

There are many research studies analyzing the performance of the energy supply system based on the PEM electrolyzer. Moharamian et al. [26] presented a biomass and natural gas fired combined cycle, the PEM electrolyzer was adopted for hydrogen production, and advanced exergy and advanced exergoeconomic methods were applied to analyze the system performances. Gholamian et al. [27] compared and studied the different geothermal-based organic Rankine cycles combined with a thermoelectric generator and a PEM electrolyzer. The optimized results indicated that the proposed novel systems showed better performances in terms of exergy efficiency and specific product cost. Taheri et al. [28] carried out the energy, exergy and economic evaluations of the multigeneration energy system for power, cooling and hydrogen, which was composed of the biomass gasification based gas turbine cycle, Rankine cycle, absorption refrigeration system and PEM electrolyzer. The fuel flow rate and gas turbine inlet temperature had an important effect on the system performance. Siddiqui and Dincer [29] developed and investigated a novel solar tower based integrated system for desalination, electricity, and hydrogen; the results indicated that the total energy and exergy efficiencies of the proposed system of 23.2% and 6.2%, respectively, can be reached.

1.3. Exergoeconomic analysis

The exergoeconomic analysis method considers both exergy and economic assessments; the related factors are adopted to obtain the evaluation of both system and equipment [30]; this method has been applied to analyze and optimize various energy supply systems. In the conventional exergoeconomic analysis, the common product cost allocation methods are mainly composed of the extraction method, equivalent method and by-product method [31], which promote the development of the exergoeconomic analysis. Ghaebi et al. [32] made an exergoeconomic analysis of a cogeneration system integrated with the organic Rankine cycle and PEM electrolyzer. It was found that R245fa was the most cost-efficient working fluid with an electricity cost of 11.54$/GJ and hydrogen cost of 4.921$/GJ, and most components had a high exergoeconomic factor. Baghernejad et al. [33] assessed the exergetic and exergoeconomic performances of three different trigeneration systems considering the multi-objective optimization issue; in addition, the effects of the key parameters on unit cost of products were also studied. Moreover, Anvari et al. [34] studied the trigeneration system performances using conventional and advanced exergoeconomic analysis and found that the comparison studies could provide more valuable information for integrated system improvement.

With the energy utilization processes proceeding, the irreversible loss gradually increases, and the related energy quality decreases accordingly [35,36]. For flue gas utilization, when a high temperature and pressure flue gas flows into the gas turbine (for power), absorption chiller (for cooling), and heat exchanger (for domestic hot water) and then discharges into the environment, the energy quality of the inlet flue gas of heat exchanger is higher than that of the outlet as the temperature of flue gas decreases. According to the principle of good quality and high price, with the decrease in the energy quality, the related unit cost decreases, and vice versa [35]. In the exergoeconomic analysis, the unit exergy cost of streams should increase with the increasing energy quality of streams, and the relationship between the unit exergy cost and energy quality is assumed to be linear [37–39]. With the appearance of more complex polygeneration systems, the products have also diversified besides the conventional electricity, heating and cooling. Therefore, the product cost allocation becomes increasingly important during the exergoeconomic analysis and optimization of the polygeneration system. Hence, it is imperative to adopt an indicator to evaluate the different types of energy. An energy level is the reflection of the energy quality in the thermodynamic processes, which is proposed by Ishida [40] and widely developed by other researchers [41–43]. As an intensive parameter, the energy level is defined as the ratio of exergy change to enthalpy change. The energy level can be used to assess the ability of the energy flow converting into available work; it can not only reflect the physical energy but also chemical energy. Therefore, the energy level based cost allocation method is adopted in the modified exergoeconomic analysis. Some researchers investigated the exergoeconomic analysis of the energy system in terms of energy level. Qi et al. [36] proposed an energy level based cost allocation method and applied to a typical CCHP system. The function relation between the unit exergy cost and energy level was established to obtain the cost allocation equations. The results showed that the novel method provided a reasonable way for evaluating the system performance. Wang et al. [37,44] compared the conventional and energy level based exergoeconomic performances of the proposed CCHP system and analyzed the off-design performances. Moreover, Wang et al. [45] conducted the exergoeconomic analysis of two biomass CCHP system, which considered the energy level in the formation of auxiliary equations, and then analyzed the reliability consideration of product cost using State-Space and Markov method [46].

According to the above literature reviews, there exist some research studies about biomass or geothermal based energy system for hydrogen production and subsequent exergoeconomic analysis, while studies on the energy level based exergoeconomic analysis of the biomass and geothermal coupling polygeneration system are relatively few. The main objectives and innovations of this research can be summarized as:

(1) A novel biomass and natural gas fired polygeneration system integrated with GSHP and PEM electrolyzer is presented for electricity, hot water, chilled water and hydrogen production.
(2) Energy level based cost allocation method is considered in the modified exergoeconomic analysis, and system performances between the conventional and energy level based exergoeconomic analysis are compared.
(3) A comprehensive sensitivity analysis is carried out to analyze the influences of the economic factors on system performances.

2. Polygeneration system description

2.1. System flowchart

The flow sheet of a novel biomass-natural gas fired polygeneration system is shown in Fig. 1. It mainly comprises of five parts: biomass gasification process, proton exchange membrane (PEM) electrolyzer, gas turbine cycle, flue gas thermal utilization and ground source heat pump (GSHP) cycle.

The biomass (stream 1, 25 °C, 1 bar) is sent into the gasifier with preheated air (stream 17, 200 °C, 1 bar), and a series of chemical reactions occur in the gasifier. The generated high-temperature bio-gas (stream 2) is first fed into HX-01 (heat exchanger) to preheat the gasify agent-air (stream 16, 25 °C, 1 bar); then, the bio-gas is further used to heat the water (stream 18, 25 °C, 1 bar) from users to a specified temperature (stream 19, 55 °C, 1 bar). Finally, the sensible heat of the bio-gas is utilized to heat the feedstock water (stream 20) of electrolysis in

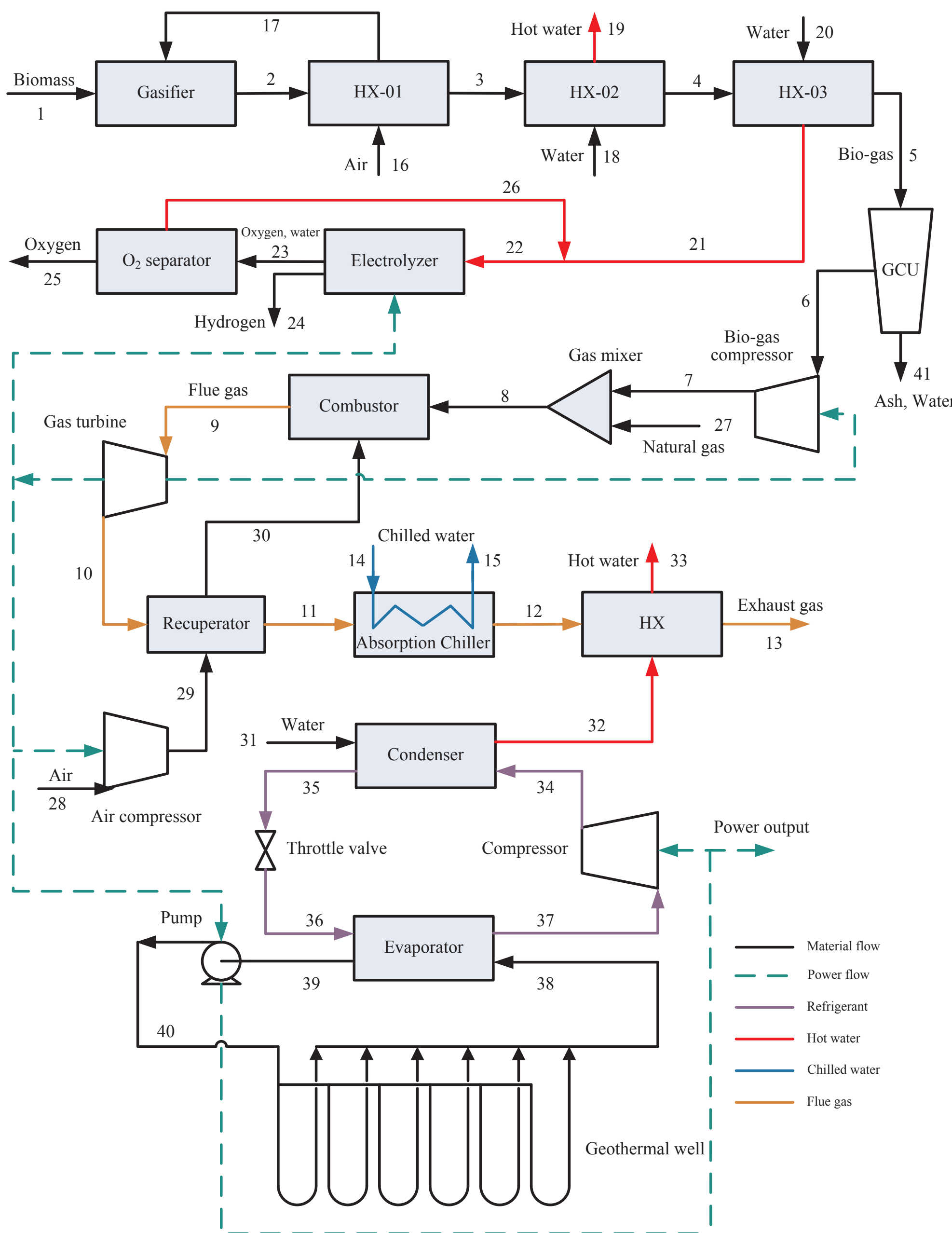

Fig. 1. Schematic diagram of proposed polygeneration system.

HX-03. After the water is heated to the electrolysis temperature (stream 21, 80 °C, 1 bar), it is fed into the electrolyzer driven by electricity and electrolyzed. The hydrogen (stream 24) derived from the cathode is stored in the tank for other applications. A mixture of un-reacted water and oxygen (stream 23) is sent into the O_2 separator, and the un-reacted hot water (stream 26) is returned to the electrolyzer for further electrolysis. After cooling and purification treatment in a gas clean unit (GCU), the bio-gas (stream 6) enters the bio-gas compressor and is compressed into a high-pressure condition (stream 7). The bio-gas and natural gas (stream 27) are mixed in the gas mixer; this measure can improve the electricity generation performance of the gas turbine cycle. The mixture gas (stream 8) is fed into the combustion reaction with compressed and preheated air (stream 30) in a combustor. The high pressure and temperature flue gas (stream 9) is converted into electricity in the gas turbine, and the power-consuming equipment in the proposed system is provided by gas turbine. In order to further improve the gas turbine performance, the compressed air (stream 29) is preheated by the flue gas in a recuperator.

Then the flue gas (stream 11) is first fed into the absorption chiller to generate chilled water (stream 15), and utilized to reheat the warm water (stream 32) in HX. After heat exchanging, the flue gas discharges into the environment at a temperature of 120 °C (stream 13). The GSHP is adopted to generate warm water: First, the refrigerant (stream 34) derived from the compressor releases the heat in hot side of the condenser, and the water (stream 31) is preheated. Then, the refrigerant (stream 35) is throttled and pressure is reduced in the throttle valve, which converts the refrigerant into gas-liquid phase region. The refrigerant (stream 36) absorbs the geothermal energy from the geothermal well and is heated into a saturated vapor condition (stream 37). Finally, the refrigerant is compressed into a high pressure and superheated condition in the compressor.

2.2. Thermodynamic analysis

The performances of proposed polygeneration system are modeled and calculated by Aspen Plus process simulator and Matlab software. The related parameters are presented in Tables 1 and 2. The following assumptions are considered in this study:

- The system operates under steady state condition;
- The pressure and temperature losses are neglected;
- The variations of kinetic and potential exergy are not considered;
- The bio-gas is composed of H_2, CO, CO_2, CH_4, H_2O, and tar formation is disregarded;
- The environmental conditions: temperature (25 °C) and pressure (1 bar).

In the proposed system, the biomass-air gasification process is considered to generate the bio-gas; the whole gasification process can be divided into a series of sub-processes: drying, pyrolysis, gasification, etc. The thermodynamic equilibrium model is used in the Aspen Plus software simulator; the above sub-processes can be represented by different reactors or components [50]. For the gas turbine cycle, the mass ratio of the bio-gas to natural gas is assumed to be 2, and the recuperator is adopted in order to increase the inlet temperature of the air in combustor, which can further utilize the waste heat of the flue gas and improve the cycle performances. For the flue gas thermal utilization, this study selects the double-effect Li-Br absorption chiller to provide chilled water (7 °C), the coefficient of performance (COP) of the absorption chiller is assumed to be constant. In the GSHP subsystem, R22 is considered as the refrigerant. The temperature of hot water is first upgraded into a mid value (39 °C) in the condenser and then reheated into the requirement temperature (55 °C) in HX. This measure contributes to decreasing the compressed ratio and improving the COP of the GSHP. The detailed descriptions of these models have been investigated in our previous research [20]. In this section, the model of the PEM electrolyzer is mainly analyzed. The electrolysis reaction contains electrochemical and thermal processes simultaneously, it can be divided into two steps: anode half reaction and cathode half reaction as the following equations presented, respectively.

$$H_2O \rightarrow 2H^+ + \frac{1}{2}O_2 + 2e^+ \tag{1}$$

$$2H^+ + 2e^+ \rightarrow H_2 \tag{2}$$

The PEM electrolyzer is driven by electricity derived from gas turbine, it is imperative to calculate the energy demand of electrolytic process, which can be determined as [49,51]:

$$\triangle H = \triangle G + T\triangle S \tag{3}$$

where $\triangle G$ is the change of Gibbs free energy or electrical energy demand of electrolysis, kJ; $T\triangle S$ is the thermal energy demand, kJ. The above values can be determined by calculating enthalpy, entropy and Gibbs free energy of water, hydrogen and oxygen, respectively. Besides that, the flow rate of products and reactants can also be calculated according to Faraday's laws and reaction stoichiometry of electrolysis [49,51]:

$$\dot{N}_{H_2,out} = \frac{J}{2F}\eta_F = \dot{N}_{H_2O,reacted} \tag{4}$$

$$\dot{N}_{O_2,out} = \frac{J}{4F}\eta_F \tag{5}$$

$$\dot{N}_{H_2O,out} = \dot{N}_{H_2O,in} - \frac{J}{2F}\eta_F \tag{6}$$

where $\dot{N}_{H_2,out}$ is the molar flow rate of generated hydrogen, mol/s; $\dot{N}_{H_2O,reacted}$ is the molar flow rate of reacted water, mol/s; $\dot{N}_{O_2,out}$ is the molar flow rate of generated oxygen, mol/s; $\dot{N}_{H_2O,out}$ is the molar flow rate of un-reacted water, mol/s; $\dot{N}_{H_2O,in}$ is the molar flow rate of input water, mol/s; J is the current density, A/m^2; F is the Faraday constant, 96,486C/mol; η_F is the Faraday efficiency. In this study, the Faraday efficiency is assumed to be 100% since this value exceeds to 99% in many literatures [52,53].

The electricity required by PEM electrolyzer can be defined as:

$$E_{ele} = JA_{cell}N_{cell}V \tag{7}$$

$$V = V_0 + V_{act,a} + V_{act,c} + V_{ohm} + V_{con} \tag{8}$$

where A_{cell} is the effective cell area (m^2), the surface area of PEM electrolyzer is assumed to be 1 m^2; N_{cell} is the number of cells; V_0 is the reversible potential, V; $V_{act,a}$ is the anode activation overpotential, V; $V_{act,c}$ is the cathode activation overpotential, V; V_{ohm} is the ohmic overpotential, V; V_{con} is the concentration overpotential, V. When the current density of PEM electrolyzer is not too high (i.e. $J < 10{,}000$ A/m^2), the concentration overpotential can be neglected [54,55]. The reversible potential can be calculated by Nernst equation:

$$V_0 = 1.229 - 8.5 \times 10^{-4}(T_{PEM} - 298) \tag{9}$$

where T_{PEM} is the electrolytic temperature, K.

Based on the ohm law, the ohmic overpotential is expressed as:

$$V_{ohm} = JR_{PEM} \tag{10}$$

where R_{PEM} is the overall ohmic resistance, Ω, which can be calculated

Table 1
Properties of biomass material [47].

Items	Parameters				
Ultimate analysis (dry basis) (wt%)	C	H	O	N	S
	39.78	4.97	40.02	0.46	0.20
Proximate analysis (dry basis) (wt%)	Volatile matter	Fixed carbon	Ash	Moisture	
	70.36	15.07	14.56	14.43	
HHV (MJ/kg)	14.144				

Table 2
Main parameters of polygeneration system [8,20,48,49].

NO.	Items	Value	Unit
Biomass gasification			
1	Flow rate of biomass	700	kg/h
2	Gasification temperature	888	°C
3	Gasification pressure	1	bar
4	Equivalence ratio	0.35	–
5	Preheated temperature of air	200	°C
6	Air pressure	1	bar
7	Temperature of hot water	55	°C
Proton exchange membrane (PEM) electrolyzer			
8	Electrolysis temperature	80	°C
9	Membrane thickness	100	μm
10	Activation energy of anode	76	kJ/mol
11	Activation energy of cathode	18	kJ/mol
12	Pre-exponential factor of anode	1.7×10^5	A/m^2
13	Pre-exponential factor of cathode	4.6×10^3	A/m^2
14	Water content of anode-membrane interface	14	–
15	Water content of cathode-membrane interface	10	–
16	Number of cells	50	–
Gas turbine cycle			
17	Pressure of natural gas	14	bar
18	Mass ratio of bio-gas to natural gas	2	–
19	Compression ratio of bio-gas compressor	13.5	–
20	Compression ratio of air compressor	13.5	–
21	Isentropic efficiency of bio-gas compressor	0.85	–
22	Mechanical efficiency of bio-gas compressor	0.99	–
23	Isentropic efficiency of air compressor	0.82	–
24	Mechanical efficiency of air compressor	0.99	–
25	Inlet temperature of gas turbine	1150	°C
26	Isentropic efficiency of gas turbine	0.87	–
27	Mechanical efficiency of gas turbine	0.99	–
28	Preheated temperature of air in recuperator	500	°C
Flue gas thermal utilization			
29	COP of absorption chiller	1.2	–
30	Outlet temperature of chilled water	7	°C
31	Inlet temperature of chilled water	12	°C
32	Temperature of hot water	55	°C
33	Outlet temperature of flue gas in chiller	200	°C
34	Temperature of exhaust gas	120	°C
Ground source heat pump (GSHP) cycle			
35	Temperature of cold water	25	°C
36	Temperature of warm water	39	°C
37	Source water outlet temperature from geothermal well	12	°C
38	Source water inlet temperature from geothermal well	7	°C

as:

$$R_{PEM} = \int_0^L \frac{dx}{\sigma_{PEM}[\lambda(x)]} \tag{11}$$

where L is the membrane thickness, μm; $\sigma_{PEM}[\lambda(x)]$ is the local ionic conductivity, s/m, it can be calculated by empirical equation [49]:

$$\sigma_{PEM}[\lambda(x)] = [0.5139\lambda(x) - 0.326]\exp\left[1268\left(\frac{1}{303} - \frac{1}{T_{PEM}}\right)\right] \tag{12}$$

where $\lambda(x)$ is the water content at location of x in membrane, Ω^{-1}, it can be calculated as:

$$\lambda(x) = \frac{\lambda_a - \lambda_c}{L}x + \lambda_c \tag{13}$$

where λ_a and λ_c is the water content at the anode-membrane interface and cathode-membrane interface, Ω^{-1}.

The activation overpotential of electrode can be expressed as [49]:

$$V_{act,i} = \frac{RT}{F}\sinh^{-1}\left(\frac{J}{2J_{0,i}}\right) = \frac{RT}{F}\ln\left[\frac{J}{2J_{0,i}} + \sqrt{\left(\frac{J}{2J_{0,i}}\right)^2 + 1}\right], \quad i = a, c \tag{14}$$

where R is the universal gas constant, kJ/(kmol·K); $J_{0,i}$ is the exchange current density, A/m^2, it can be calculated as:

$$J_{0,i} = J_i^{ref}\exp\left(-\frac{E_{act,i}}{RT}\right), \quad i = a, c \tag{15}$$

where J_i^{ref} is the pre-exponential factor, A/m^2; $E_{act,i}$ is the activation energy of anode or cathode, kJ/mol.

3. Conventional and modified exergoeconomic method

3.1. Exergy cost equations

According to the method of Specific Exergy Costing (SPECO) and the F-P principle (fuel-product) [56,57], the exergy cost balance equation of equipment in energy system can be expressed as [58]:

$$\sum (c_p EX_p)_k = \sum (c_f EX_f)_k + \dot{Z}_k \tag{16}$$

$$\dot{C} = c\cdot EX \tag{17}$$

where EX_f, EX_p represents the fuel exergy and product exergy of k-th equipment, respectively, kW; c represents the cost per unit exergy of streams, including material, heat or work flows, \$/kWh; $\dot{C}$ represents the cost rate of streams, \$/h; $\dot{Z}_k$ represents the investment cost rate of k-th equipment, \$/h. The investment cost rate consists of two parts: annual levelized capital investment ($\dot{Z}_{CI,k}$) and annual levelized operation and maintenance cost ($\dot{Z}_{OM,k}$), which can be determined as [13,59]:

$$\dot{Z}_k = \dot{Z}_{CI,k} + \dot{Z}_{OM,k} \tag{18}$$

For the annual levelized capital investment of k-th equipment, it can be expressed as [13,59]:

$$\dot{Z}_{CI,k} = \left(\frac{CRF}{\tau}\right)\cdot Z_k \tag{19}$$

$$CRF = \frac{P(1+P)^n}{(1+P)^n - 1} \tag{20}$$

where Z_k is the capital investment cost of k-th equipment, which are presented in Table 3, \$; τ is the annual operating hours, h; CRF is the capital recovery factor, P is the interest rate, %; n is the service life.

For the annual levelized operation and maintenance of k-th equipment, it can be expressed as:

$$\dot{Z}_{OM,k} = \frac{\lambda}{\tau}\cdot Z_k \tag{21}$$

where λ is the ratio of operation and maintenance cost to capital investment cost of equipment, %.

3.2. Comparison of conventional and modified cost allocation

To calculate the cost per exergy unit of different streams in the proposed system, the auxiliary cost equations of different equipment are needed. The exergy cost balance equations of different equipment between conventional and modified exergoeconomic analysis are the same, and so are the capital investment costs of different equipment. The main and core distinction between conventional and modified exergoeconomic analysis lies in the difference of cost allocation, that is the auxiliary cost equation for different equipment.

In the conventional exergy cost allocation, the conventional auxiliary cost allocation equations can be listed in Table 4 (the second column) according to the F-P principles in reference [56]. For the heat exchanger (HX-01, HX-02, HX-03, recuperator, condenser, and evaporator), absorption chiller, and gas turbine, the unit exergy costs of inlet and outlet streams are equivalent. For the bio-gas compressor, air compressor, compressor, and pump, the unit exergy cost of the inlet power is equal to the unit exergy cost of the power generated by the gas turbine.

Table 3
Exergy cost balances equation and capital investment cost of system equipment [60,61].

Component	Exergy cost balance equation	Capital investment cost
Gasifier	$\dot{C}_2 = \dot{C}_1 + \dot{C}_{17} + \dot{Z}_G$	$Z_G = 1600(\dot{m}_{biomass}[kg/h])^{0.67}$
HX-01	$\dot{C}_{17} - \dot{C}_{16} = \dot{C}_2 - \dot{C}_3 + \dot{Z}_{HX-01}$	$Z_{HX-01} = 130\left(\frac{S_{HX-01}}{0.093}\right)^{0.78}$
HX-02	$\dot{C}_{19} - \dot{C}_{18} = \dot{C}_3 - \dot{C}_4 + \dot{Z}_{HX-02}$	$Z_{HX-02} = 130\left(\frac{S_{HX-02}}{0.093}\right)^{0.78}$
HX-03	$\dot{C}_{21} - \dot{C}_{20} = \dot{C}_4 - \dot{C}_5 + \dot{Z}_{HX-03}$	$Z_{HX-02} = 130\left(\frac{S_{HX-02}}{0.093}\right)^{0.78}$
Electrolyzer	$\dot{C}_{23} + \dot{C}_{24} = \dot{C}_{W_{PEM}} + \dot{C}_{22} + \dot{Z}_{PEM}$	$Z_{PEM} = 1000W_{PEM}$
GCU	$\dot{C}_6 = \dot{C}_5 + \dot{Z}_{GCU}$	$Z_{GCU} = 0.05 \times 1600(\dot{m}_{biomass}[kg/h])^{0.67}$
Bio-gas compressor	$\dot{C}_7 - \dot{C}_6 = \dot{C}_{W_{GC}} + \dot{Z}_{GC}$	$Z_{GC} = \frac{N_{11}\dot{m}_{bio-gas}}{N_{12} - \eta_{is,GC}} r_p \ln(r_p) N_{11} = 71.1\$/(kg/s),\ N_{12} = 0.9$
Gas mixer	$\dot{C}_8 = \dot{C}_7 + \dot{C}_{27} + \dot{Z}_{GM}$	$Z_{GM} = 0$
Air compressor	$\dot{C}_{29} - \dot{C}_{28} = \dot{C}_{W_{AC}} + \dot{Z}_{AC}$	$Z_{AC} = \frac{N_{21}\dot{m}_{air}}{N_{22} - \eta_{is,AC}} r_p \ln(r_p) N_{21} = 71.1\$/(kg/s)\quad N_{22} = 0.9$
Combustor	$\dot{C}_9 = \dot{C}_8 + \dot{C}_{30} + \dot{Z}_C$	$Z_{COM} = \frac{N_{31}\dot{m}_{air}}{N_{32} - 0.98}(1 + \exp(N_{33}T_{COM} - N_{34}))$ $N_{31} = 46.08,\ N_{32} = 0.995,\ N_{33} = 0.018,\ N_{34} = 26.4$
Gas turbine	$\dot{C}_{W_{GT}} = \dot{C}_9 - \dot{C}_{10} + \dot{Z}_{GT}$	$Z_{GT} = \frac{N_{41}\dot{m}_{23}}{N_{42} - \eta_{is,GT}} \ln\left(\frac{P_8}{P_9}\right)(1 + \exp(N_{43}T_8 - N_{44}))$ $N_{41} = 479.34,\ N_{42} = 0.92,\ N_{43} = 0.036\quad N_{44} = 54.4$
Recuperator	$\dot{C}_{30} - \dot{C}_{29} = \dot{C}_{10} - \dot{C}_{11} + \dot{Z}_{REC}$	$Z_{REC} = 130\left(\frac{S_{REC}}{0.093}\right)^{0.78}$
Absorption chiller	$\dot{C}_{15} - \dot{C}_{14} = \dot{C}_{11} - \dot{C}_{12} + \dot{Z}_{AB}$	$Z_{AB} = 196 \times Q_{AB}$
HX	$\dot{C}_{33} - \dot{C}_{32} = \dot{C}_{12} - \dot{C}_{13} + \dot{Z}_{HX}$	$Z_{HX} = 130\left(\frac{S_{HX}}{0.093}\right)^{0.78}$
Condenser	$\dot{C}_{32} - \dot{C}_{31} = \dot{C}_{34} - \dot{C}_{35} + \dot{Z}_{CON}$	$Z_{CON} = 8000\left(\frac{A_{CON}}{100}\right)^{0.6}$
Throttle valve	$\dot{C}_{36} = \dot{C}_{35} + \dot{Z}_{VAL}$	$Z_{VAL} = 0$
Evaporator	$\dot{C}_{39} - \dot{C}_{38} = \dot{C}_{36} - \dot{C}_{37} + \dot{Z}_{EVA}$	$Z_{EVA} = 16000\left(\frac{S_{EVA}}{100}\right)^{0.6}$
Compressor	$\dot{C}_{34} - \dot{C}_{37} = \dot{C}_{W_{COM}} + \dot{Z}_{COM}$	$Z_{COM} = \frac{N_{51}\dot{m}_{refrigerant}}{N_{52} - \eta_{is,COM}} r_p \ln(r_p)$ $N_{51} = 39.5\$/(kg/s),\ N_{52} = 0.9$
Pump	$\dot{C}_{40} - \dot{C}_{39} = \dot{C}_{W_P} + \dot{Z}_P$	$Z_P = 800\left(\frac{W_P}{10}\right)^{0.26}\left(\frac{1-\eta_P}{\eta_P}\right)^{0.5}$
Geothermal well[a]	$\dot{C}_{38} - \dot{C}_{40} = \dot{C}_{GW} + \dot{Z}_{GW}$	$Z_{GW} = 2900N_{GW}$

[a] The capital investment cost of geothermal well mainly refers to the capital investment cost of ground heat exchanger. In the practical engineering, the pipe length can be calculated by heat exchanger rate for the borehole heat exchanger per meter length, and then the borehole number (N_{GW}) can be calculated according to drilling depth and type of vertical buried pipe [62]. The heat exchanger rate for the borehole heat exchanger per meter length is about 45 W/m, which is obtained according to the testing parameters of geothermal properties in Changsha, China; and the borehole cost (it mainly consists of drilling cost, construction cost, material expense, etc.) is about 2900$ according to local market quotation. Moreover, in order to obtain the soil heat, there is no other purchased cost besides the capital investment cost of geothermal well, therefore the purchased cost of soil heat ($\dot{C}_{GW}$) is assumed to be zero.

For the modified exergy cost allocation, due to the distinction of temperature the energy level of inlet stream is not equal to the energy level of the same stream existed from equipment. For example, the energy level of the inlet flue gas in the gas turbine, absorption chiller, and HX is higher than the energy level of outlet streams. According to the economic principle, a good quality of stream has a high price. Therefore, the unit exergy cost of the streams should be proportional to their energy level, and the conventional cost allocation equation can be modified as:

$$\frac{c_m}{A_m} = \frac{c_n}{A_n} \quad or \quad \frac{\dot{C}_m/EX_m}{A_m} = \frac{\dot{C}_n/EX_n}{A_n} \tag{22}$$

where A_m, A_n represents the energy level of each stream. Energy level mainly stands for the energy quality of stream and the ability of transforming different energy into useful work [63]. It can be expressed as:

$$A = \frac{dE}{dH} = 1 - T_0\left(\frac{dS}{dH}\right) \tag{23}$$

where dE, dH and dS represent the exergy change, enthalpy change and entropy change, respectively; T_0 represents the environmental temperature, K.

Additionally, some supplementary equations should be also considered, the cost of air and water, such as stream 16, 18, 20 and 31, are equal to zero. The cost of biomass and natural gas can be calculated as:

$$C_1 = c_1 EX_1 = c_{biomass} m_{biomass} \tag{24}$$

$$C_{27} = c_{27} EX_{27} = c_{natural\ gas} m_{natural\ gas} \tag{25}$$

where $c_{biomass}$, $c_{natural\ gas}$ represents the price of biomass and natural gas, respectively; $m_{biomass}$, $m_{natural\ gas}$ represents the mass flow rate of biomass and natural gas, respectively, kg/h. The economic parameters can be seen from Table 5.

4. System performance calculation

4.1. Evaluation criteria

The thermodynamic analysis has been investigated in Section 2.2, the related evaluation indicators should be considered. The overall energy efficiency and exergy efficiency can be expressed as:

$$\eta_{en} = \frac{Q_{CHP} + Q_{GSHP} + Q_C + E_{GT} + LHV_{H_2}\dot{m}_{H_2}}{LHV_{biomass}\dot{m}_{biomass} + LHV_{natural\ gas}\dot{m}_{natural\ gas}} \times 100\% \tag{26}$$

Table 4
Auxiliary cost equation of system equipment.

Component	Conventional equation	Modified equation
Gasifier	–	–
HX-01	$\frac{\dot{C}_2}{EX_2}=\frac{\dot{C}_3}{EX_3}$	$\frac{\dot{C}_2/EX_2}{A_2}=\frac{\dot{C}_3/EX_3}{A_3}$
HX-02	$\frac{\dot{C}_3}{EX_3}=\frac{\dot{C}_4}{EX_4}$	$\frac{\dot{C}_3/EX_3}{A_3}=\frac{\dot{C}_4/EX_4}{A_4}$
HX-03	$\frac{\dot{C}_4}{EX_4}=\frac{\dot{C}_5}{EX_5}$	$\frac{\dot{C}_4/EX_4}{A_4}=\frac{\dot{C}_5/EX_5}{A_5}$
Electrolyzer	$\frac{\dot{C}_{W_{PEM}}}{W_{PEM}}=\frac{\dot{C}_{W_{GT}}}{W_{GT}+W_{AC}+W_{GC}+W_{COM}+W_{PEM}+W_P}$	$\frac{\dot{C}_{W_{PEM}}}{W_{PEM}}=\frac{\dot{C}_{W_{GT}}}{W_{GT}+W_{AC}+W_{GC}+W_{COM}+W_{PEM}+W_P}$
GCU	–	–
Bio-gas compressor	$\frac{\dot{C}_{W_{GC}}}{W_{GC}}=\frac{\dot{C}_{W_{GT}}}{W_{GT}+W_{AC}+W_{GC}+W_{COM}+W_{PEM}+W_P}$	$\frac{\dot{C}_{W_{GC}}}{W_{GC}}=\frac{\dot{C}_{W_{GT}}}{W_{GT}+W_{AC}+W_{GC}+W_{COM}+W_{PEM}+W_P}$
Gas mixer	–	–
Air compressor	$\frac{\dot{C}_{W_{AC}}}{W_{AC}}=\frac{\dot{C}_{W_{GT}}}{W_{GT}+W_{AC}+W_{GC}+W_{COM}+W_{PEM}+W_P}$	$\frac{\dot{C}_{W_{AC}}}{W_{AC}}=\frac{\dot{C}_{W_{GT}}}{W_{GT}+W_{AC}+W_{GC}+W_{COM}+W_{PEM}+W_P}$
Combustor	–	–
Gas turbine	$\frac{\dot{C}_9}{EX_9}=\frac{\dot{C}_{10}}{EX_{10}}$	$\frac{\dot{C}_9/EX_9}{A_9}=\frac{\dot{C}_{10}/EX_{10}}{A_{10}}$
Recuperator	$\frac{\dot{C}_{10}}{EX_{10}}=\frac{\dot{C}_{11}}{EX_{11}}$	$\frac{\dot{C}_{10}/EX_{10}}{A_{10}}=\frac{\dot{C}_{11}/EX_{11}}{A_{11}}$
Absorption chiller	$\frac{\dot{C}_{11}}{EX_{11}}=\frac{\dot{C}_{12}}{EX_{12}}$	$\frac{\dot{C}_{11}/EX_{11}}{A_{11}}=\frac{\dot{C}_{12}/EX_{12}}{A_{12}}$
HX	$\frac{\dot{C}_{12}}{EX_{12}}=\frac{\dot{C}_{13}}{EX_{13}}$	$\frac{\dot{C}_{12}/EX_{12}}{A_{12}}=\frac{\dot{C}_{13}/EX_{13}}{A_{13}}$
Condenser	$\frac{\dot{C}_{34}}{EX_{34}}=\frac{\dot{C}_{35}}{EX_{35}}$	$\frac{\dot{C}_{34}/EX_{34}}{A_{34}}=\frac{\dot{C}_{35}/EX_{35}}{A_{35}}$
Throttle valve	–	–
Evaporator	$\frac{\dot{C}_{38}}{EX_{38}}=\frac{\dot{C}_{39}}{EX_{39}}$	$\frac{\dot{C}_{38}/EX_{38}}{A_{38}}=\frac{\dot{C}_{39}/EX_{39}}{A_{39}}$
Compressor	$\frac{\dot{C}_{W_{COM}}}{W_{COM}}=\frac{\dot{C}_{W_{GT}}}{W_{GT}+W_{AC}+W_{GC}+W_{COM}+W_{PEM}+W_P}$	$\frac{\dot{C}_{W_{COM}}}{W_{COM}}=\frac{\dot{C}_{W_{GT}}}{W_{GT}+W_{AC}+W_{GC}+W_{COM}+W_{PEM}+W_P}$
Pump	$\frac{\dot{C}_{W_P}}{W_P}=\frac{\dot{C}_{W_{GT}}}{W_{GT}+W_{AC}+W_{GC}+W_{COM}+W_{PEM}+W_P}$	$\frac{\dot{C}_{W_P}}{W_P}=\frac{\dot{C}_{W_{GT}}}{W_{GT}+W_{AC}+W_{GC}+W_{COM}+W_{PEM}+W_P}$
Geothermal well	–	–

Table 5
The economic values of polygeneration system [64].

Parameter	Value	Unit
Interest rate	10	%
Service life	20	year
Operation and maintenance cost ratio	6	%
Operating hours	7446	h
Biomass	57.2	\$/ton
Natural gas	0.528	\$/m^3

$$\eta_{ex}=\frac{EX_{\text{hot water}}+EX_{\text{C}}+E_{\text{GT}}+ex_{\text{H}_2}\dot{m}_{\text{H}_2}}{LHV_{\text{biomass}}\dot{m}_{\text{biomass}}+LHV_{\text{natural gas}}\dot{m}_{\text{natural gas}}}\times 100\% \tag{27}$$

where Q_{CHP}, Q_{GSHP} represent the heating generated by gas turbine cycle and ground source heat pump cycle, respectively, kW; E_{GT} represents the electricity generated by proposed system, kW; Q_{C} represents the cooling generated by proposed system, kW; $EX_{\text{hot water}}$ represents the exergy of hot water generated by proposed system, kW; EX_{C} represents the exergy of cooling generated by proposed system, kW; LHV_{H_2}, ex_{H_2}, $\dot{m}_{\text{H}_2}$ represent the lower heating value, specific chemical exergy and mass flow rate of hydrogen, respectively; LHV_{biomass}, $\dot{m}_{\text{biomass}}$ represent the lower heating value and mass flow rate of biomass, respectively; $LHV_{\text{natural gas}}$, $\dot{m}_{\text{natural gas}}$ represent the lower heating value and mass flow rate of natural gas, respectively.

For the PEM electrolyzer, the energy and exergy efficiency can be defined as:

$$\eta_{en,PEM}=\frac{LHV_{\text{H}_2}\dot{m}_{\text{H}_2}}{E_{\text{PEM}}+Q_{\text{heat,PEM}}+Q_{\text{H}_2O}}\times 100\% \tag{28}$$

$$\eta_{ex,PEM}=\frac{ex_{\text{H}_2}\dot{m}_{\text{H}_2}}{E_{\text{PEM}}+EX_{\text{heat,PEM}}+EX_{\text{H}_2O}}\times 100\% \tag{29}$$

where E_{PEM}, $Q_{\text{heat,PEM}}$ represent the required electricity and heat for PEM electrolyzer, respectively, kW; $EX_{\text{heat,PEM}}$ represents the exergy of required heat for PEM electrolyzer, kW; $EX_{\text{H}_2\text{O}}$, Q_{H_2O} represent the exergy and thermal energy for heating the H_2O to electrolytic temperature, respectively, kW;

In addition, the exergoeconomic parameters should also be considered to analyze the system performance, such as exergoeconomic factor, relative cost difference. The exergoeconomic factor is defined as the ratio of investment cost to total cost (investment, exergy destruction and loss cost), it can reflect the relative importance of capital cost and exergy destruction or loss. The relative cost difference indicates the relative increase in average cost per exergy unit between fuel and product streams in different equipment; it can be used to optimize the equipment performance. These two indicators can be expressed as:

$$f_k=\frac{\dot{Z}_{\text{k}}}{\dot{Z}_{\text{k}}+\dot{C}_{\text{D,k}}+\dot{C}_{\text{L,k}}} \tag{30}$$

$$r_k=\frac{c_{\text{p,k}}-c_{\text{f,k}}}{c_{\text{f,k}}} \tag{31}$$

where $\dot{C}_{\text{D,k}}$, $\dot{C}_{\text{L,k}}$ represent the cost rate associated with exergy destruction and exergy loss in equipment, respectively, \$/h; $c_{\text{f,k}}$, $c_{\text{p,k}}$ represent unit exergy cost of fuel and product in equipment, respectively, \$/GJ.

The unit exergy cost of products of polygeneration system can be determined as:

$$c_{hot\ water,HX-02}=\frac{\dot{C}_{19}}{EX_{19}} \tag{32}$$

$$c_{hot\ water,HX}=\frac{\dot{C}_{33}}{EX_{33}} \tag{33}$$

$$c_{chilled\ water}=\frac{\dot{C}_{15}-\dot{C}_{14}}{EX_{15}-EX_{14}} \tag{34}$$

$$c_{electricity} = \frac{\dot{C}_{WGT}}{W_{GT} + W_{AC} + W_{GC} + W_{COM} + W_{PEM} + W_P} \tag{35}$$

$$c_{H_2} = \frac{\dot{C}_{24}}{EX_{24}} \tag{36}$$

4.2. Calculation results

Table 6 presents the calculation results of proposed polygeneration system. In the design condition, the input mass flow rate of biomass and natural gas are 700 kg/h and 785 kg/h, respectively; the outputs of electricity, hot water, chilled water and hydrogen are 3636.0 kW, 2896.6 kW, 5860.0 kW and 11.2 kg/h, respectively. When the current density of PEM electrolyzer keeps at the value of 5000 A/m^2, the energy and exergy efficiency of electrolysis can be reached at 58.09% and 57.58%, respectively; the energy and exergy efficiency of polygeneration system are 94.93% and 31.62%, respectively. The ratio of heat to power is 0.67, which is lower than the ratio of cooling to power. Moreover, the total investment cost of proposed system can be reached at about 4,013,843 $.

5. Discussion

5.1. Validation of PEM electrolyzer

The simulated results of the present study are compared with the experimental results investigated by Ioroi et al. [65] to validate the effectiveness of the PEM electrolyzer model. As depicted in Fig. 2, the results obtained using the present model agree well with the results reported in the literature. The cell voltage increases sharply when the current density varies from 0 to 300 A/m^2. Then it increases gradually with increasing current density when the current density exceeds 300 A/m^2. Fig. 3 presents the variations in the overpotentials of the PEM electrolyzer under different current densities. The variation in the anode activation overpotential is the same as that of the cell voltage shown in Fig. 2. The cathode activation overpotential increases rapidly when the current density increases from 0 to 300 A/m^2. It then increases gradually when the current density varies from 300 to 6000 A/m^2. Unlike the trends exhibited by the above parameters, the increasing range of ohmic overpotential is lower than the anode activation overpotential and cathode activation overpotential.

5.2. Thermodynamic performances

5.2.1. Effects of current density on energy and exergy efficiencies of PEM electrolyzer

The influences of current density on the energy and exergy efficiencies of the PEM electrolyzer are illustrated in Fig. 4. The efficiencies decrease rapidly when the current density increases from 0 to 500 A/m^2. The variation range gradually decreases with increasing current density. The reason behind this phenomenon is that the overpotentials (also called irrversibilities, $2F(V_0 + V_{act,a} + V_{act,c} + V_{ohm})$) are higher than the required heat ($T\triangle S$) at increased current densities, in accordance with thermodynamic analysis; therefore, no additional heat is required. The input energy for electrolysis mainly consists of electricity and thermal energy for heating water; however the contribution of thermal energy is much lower than that of electricity. On the other hand, with the increase in current density, the electricity required for electrolysis increases and H_2 production also increases accordingly. Because the growth rate of electricity input is higher than the growth rate of H_2 production, the efficiencies decrease gradually. In addition, the variation in exergy efficiency is similar to that of energy efficiency because the exergy and thermal energy of H_2 generation are similar.

5.2.2. Variations in exergy destruction and exergy efficiency of proposed system equipment

Fig. 5 illustrates the distributions of exergy destruction for different system equipment. The contribution of the combustor toward exergy destruction is the highest among all the components. It contributes more than 40% and is comfortably ahead of the second component (absorption chiller), which contributes approximately 23.07% toward the total exergy destruction. The above phenomenon derives from the high irreversibility of the combustion process and heat transfer temperature difference of absorption chiller, respectively. Because of the complexity of the chemical reaction, the gasification process results in high irreversibility, and the exergy destruction ratio of gasifier exceeds 10%. Moreover, the exergy destruction ratios of HX-02, PEM electrolyzer, air compressor, gas turbine and HX can be seen obviously, while that of ground source heat pump (condenser, throttle valve, evaporator and compressor) is less obvious. Considering the principle of energy cascade utilization, the available thermal energy of flue gas in HX is relatively low; hence, the magnitude of obtained energy in the ground source heat pump decreases subsequently.

The distributions of exergy efficiency of system equipment are presented in Fig. 6. As depicted in the picture, the gas mixer has the highest exergy efficiency, which is almost equal to 100%, followed by GCU, bio-gas compressor, air compressor, gas turbine, recuperator, and throttle valve, which exceeds 90%. HX-02 has the lowest exergy efficiency of approximately 9.7%. The exergy efficiency of the absorption chiller and HX are also lower. The exergy of products (hot water and chilled water) in these components are relatively lower owing to the low temperature of products.

5.2.3. Effects of current density on energy and exergy efficiencies of proposed system

The influences of current density on the energy and exergy efficiencies of proposed system are illustrated in Fig. 7. The energy and exergy efficiencies of the proposed system decrease with increasing current density. With the increase in the current density of the PEM electrolyzer, the production of hydrogen increases. The efficiency of the electrolyzer decreases when the increasing rate of hydrogen is lower than that of the required electricity, as shown in Fig. 4. In addition, the inputs (biomass and natural gas) and outputs (heating and cooling) are all constant; hence the energy efficiency decreases with increasing current density. Because of the low exergy of hot water and chilled water, the exergy efficiency of the proposed system is considerably lower than energy efficiency.

Table 6
Calculation results of polygeneration system.

	Item	Value	Unit
Inputs	Biomass	700	kg/h
	Natural gas	785	kg/h
	Flow rate of water for electrolysis	100	kg/h
	Flow rate of water for hot water	13,500	kg/h
	Heat derived from soil	955.9	kW
Outputs	Hot water	2896.6	kW
	Chilled water	5860.0	kW
	Hydrogen	11.2	kg/h
	Electricity	3636.0	kW
Performances	Energy efficiency of electrolysis	58.09	%
	Exergy efficiency of electrolysis	57.58	%
	Energy efficiency of proposed system	94.93	%
	Exergy efficiency of proposed system	31.62	%
	Ratio of heat to power	0.67	–
	Ratio of cooling to power	1.61	–
	Capital investment cost	4,013,843	$

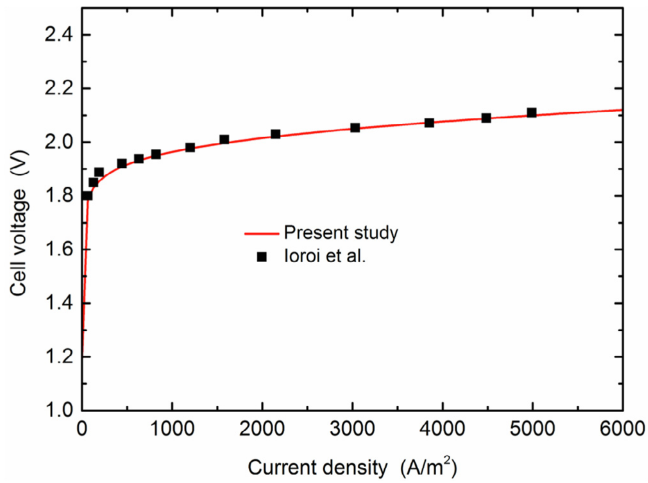

Fig. 2. Comparison of present simulated results with Ioroi et al. results for PEM electrolyzer.

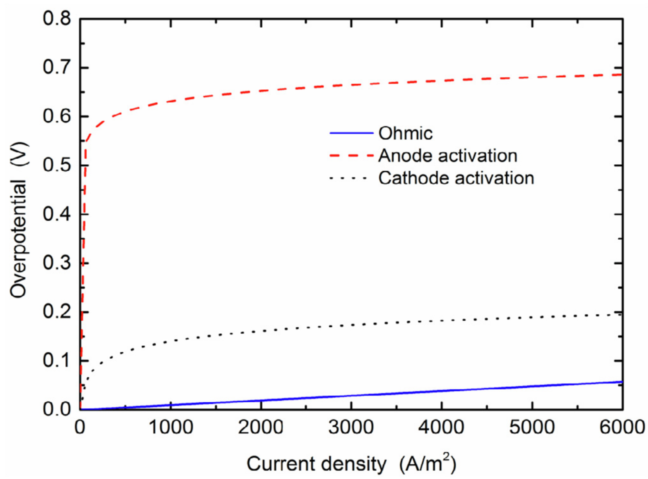

Fig. 3. Variations in overpotentials of the PEM electrolyzer under different current densities.

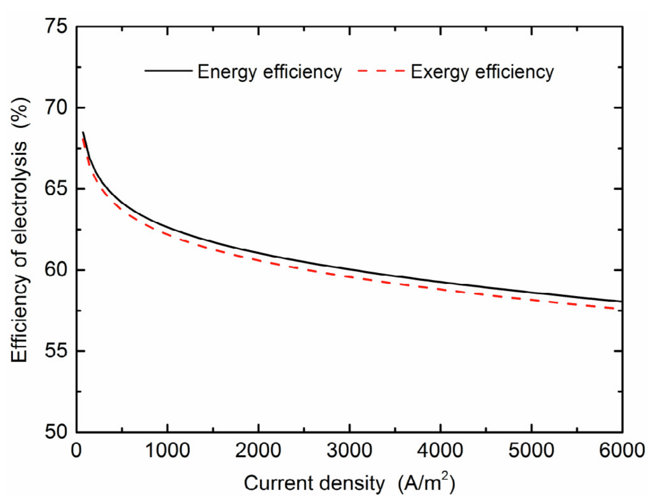

Fig. 4. Variations in energy and exergy efficiencies of the PEM electrolyzer under different current densities.

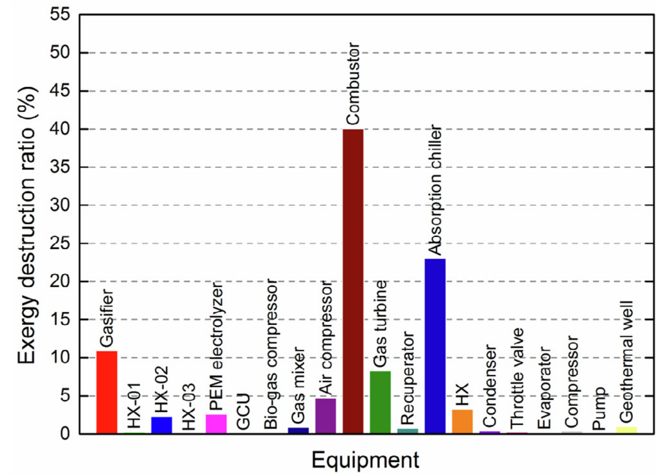

Fig. 5. Proportion of system equipment in total exergy destruction.

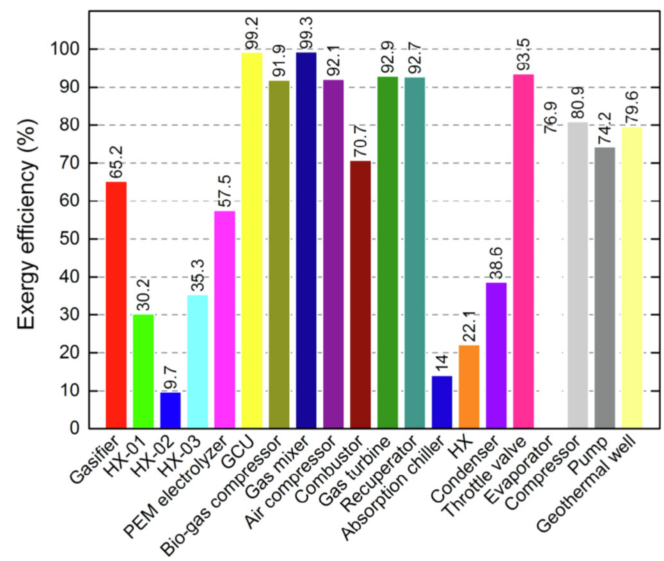

Fig.6. Distribution of exergy efficiency of system equipment.

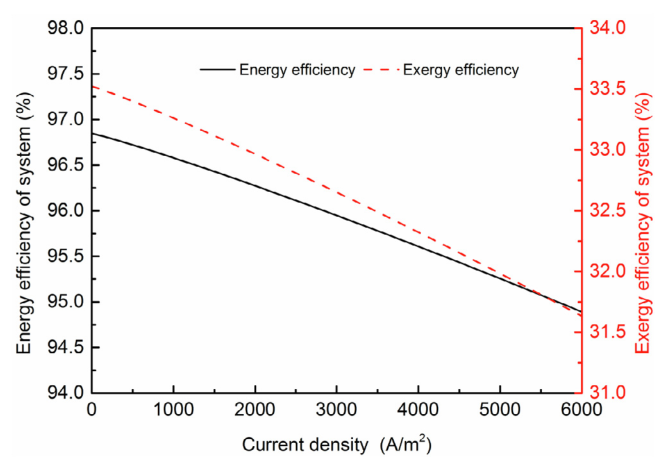

Fig. 7. Variations in energy and exergy efficiencies of proposed system under different current densities.

Table 7
The results of conventional exergoeconomic analysis for system components.

Equipment	$c_{k,f}$ ($/kWh)	$c_{k,p}$ ($/kWh)	$\dot{C}_{dest,k.}$ ($/h)	$\dot{C}_{loss,k.}$ ($/h)	$\dot{Z}_k$ ($/h)	$\dot{Z}_k + \dot{C}_{dest,k.} + \dot{C}_{loss,k.}$ ($/h)	f_k (%)	r_k (%)
Gasifier	0.0136	0.0224	14.24	0	3.07	17.31	17.74	64.83
HX-01	0.0224	0.0781	0.60	0	0.05	0.65	7.35	249.10
HX-02	0.0224	0.2439	5.02	0	0.32	5.34	6.04	990.10
HX-03	0.0224	0.1217	0.02	0	0.03	0.06	58.70	443.90
PEM electrolyzer	0.0158	0.0683	4.00	0.05	15.03	19.08	78.78	332.60
GCU	0.0224	0.0227	0.29	0	0.15	0.44	34.74	1.21
Bio-gas compressor	0.0158	0.0201	0.24	0	0.52	0.76	68.12	27.54
Gas mixer	0.0066	0.0066	0.58	0	0	0.58	0	0.67
Air compressor	0.0158	0.0204	7.22	0	17.63	24.86	70.94	29.35
Combustor	0.0066	0.0095	25.49	0	1.58	27.07	5.84	44.01
Gas turbine	0.0138	0.0158	11.05	0	9.58	20.63	46.44	14.25
Recuperator	0.0138	0.0185	1.03	0	3.44	4.46	76.99	34.04
Absorption chiller	0.0138	0.1746	30.62	0	27.37	57.99	47.20	1163.00
HX	0.0138	0.0795	4.36	4.46	1.53	10.35	14.79	475.00
Condenser	0.2738	0.7100	11.36	0	0.02	11.38	0.18	159.30
Throttle valve	0.2738	0.2928	6.85	0	0	6.85	0	6.94
Evaporator	−0.2801	−0.2156	−4.43	0	0.02	−4.41	−0.34	−23.05
Compressor	0.0158	0.0235	0.60	0	0.65	1.25	51.86	49.06
Pump	0.0158	0.0248	0.01	0	0.01	0.02	39.12	57.14
Geothermal well	0	−0.2673	0	0	14.65	14.65	100.00	Inf

Table 8
The results of modified exergoeconomic analysis for system components.

Equipment	$c_{k,f}$ ($/kWh)	$c_{k,p}$ ($/kWh)	$\dot{C}_{dest,k.}$ ($/h)	$\dot{C}_{loss,k.}$ ($/h)	$\dot{Z}_k$ ($/h0	$\dot{Z}_k + \dot{C}_{dest,k.} + \dot{C}_{loss,k.}$ ($/h)	f_k (%)	r_k (%)
Gasifier	0.0135	0.0223	14.21	0	3.07	17.28	17.78	64.86
HX-01	0.0197	0.0694	0.53	0	0.05	0.58	8.25	251.50
HX-02	0.0136	0.1537	3.05	0	0.32	3.37	9.56	1029.00
HX-03	−0.0183	0.0067	−0.02	0	0.03	0.01	236.00	−136.70
PEM electrolyzer	0.0188	0.0735	4.77	0.06	15.03	19.86	75.68	290.50
GCU	0.0237	0.0239	0.31	0	0.15	0.46	33.49	1.19
Bio-gas compressor	0.0188	0.0235	0.29	0	0.52	0.81	64.18	24.51
Gas mixer	0.0068	0.0068	0.60	0	0	0.60	0	0.68
Air compressor	0.0188	0.0237	8.61	0	17.63	26.25	67.18	25.99
Combustor	0.0068	0.0098	26.28	0	1.58	27.86	5.67	43.93
Gas turbine	0.0167	0.0188	13.31	0	9.58	22.89	41.85	13.12
Recuperator	0.0145	0.0192	1.08	0	3.44	4.51	76.15	32.84
Absorption chiller	0.0117	0.1596	25.96	0	27.37	53.33	51.33	1262.00
HX	0.0072	0.0496	2.27	2.32	1.53	6.12	24.99	588.50
Condenser	0.2829	0.7336	11.74	0	0.02	11.76	0.18	159.3
Throttle valve	−0.1277	−0.1365	−3.19	0	0	−3.19	0	6.94
Evaporator	−0.2803	−0.2157	−4.43	0	0.02	−4.41	−0.34	−23.05
Compressor	0.0189	0.0273	0.72	0	0.65	1.36	47.44	44.93
Pump	0.0189	0.0289	0.02	0	0.01	0.02	35	53.51
Geothermal well	0	−0.2673	0	0	14.65	14.65	100	Inf

5.3. Exergoeconomic performances

5.3.1. Exergoeconomic criteria analysis

Tables 7 and 8 present the exergoeconomic analysis results of system equipment for two different methods. In Table 7, the highest exergoeconomic factor is observed for the geothermal well. Because there is no other purchased cost except the capital investment cost of geothermal well, the purchased cost of soil heat is assumed to be zero. Therefore the unit exergy cost of fuel for the geothermal well is zero, and the related exergoeconomic factor is 100%. The PEM electrolyzer has the second highest exergoeconomic factor, as the investment cost rate of the PEM electrolyzer is dominant compared with that associated with exergy destruction. These situations are also observed in the recuperator, air compressor and bio-gas compressor, and the exergoeconomic factors of the above equipment are next to the PEM electrolyzer. The absorption chiller, despite having the highest investment cost rate, has a relatively low exergoeconomic factor compared with the cost of exergy destruction. Moreover, the lowest exergoeconomic factor is observed for the evaporator; condenser, combustor, HX-01, and HX-02 are followed, which shows that the costs of exergy destruction of these components are more significant compared with the capital investment cost. Therefore some measures should be adopted to decrease their exergy destruction. Similarly, as the exergy destruction of the absorption chiller and gasifier are ranked first and third among all the equipment, their exergoeconomic factors are relatively higher, and the investment cost rate of the absorption chiller and gasifier occupies a certain proportion. In addition, the unit exergy cost of product is higher than the unit exergy cost of fuel, and the relative cost differences of these components (absorption chiller, HX-01, HX-02, HX-03, PEM electrolyzer, HX and condenser) are very high, which exceed 100%. The relative cost differences among the GCU, gas mixer and throttle valve are very low because the unit exergy costs of fuel and product are similar. In general, the conventional exergoeconomic analysis is similar to the modified method, except for a few differences. The exergoeconomic factors of the gasifier, HX-01, HX-02. HX-03, absorption chiller, and HX under the modified method are slightly higher than that under the conventional method, and the exergoeconomic factors of other equipment under the modified method are lower than that under the conventional method.

5.3.2. Proportion of proposed system equipment in capital investment cost

Fig. 8 shows the distribution of capital investment cost of system

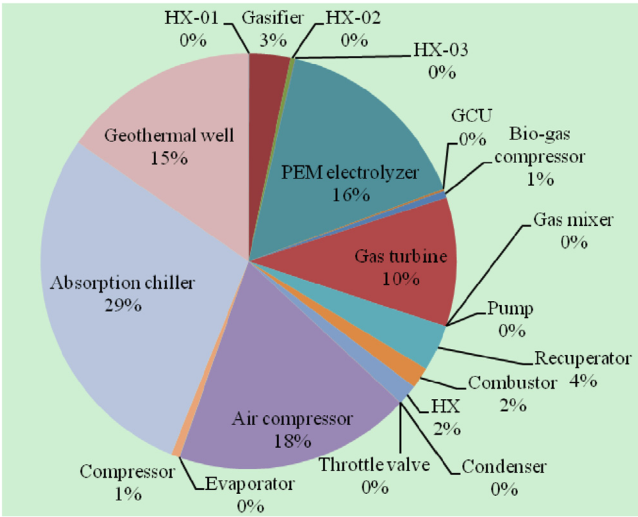

Fig. 8. Distribution of capital investment cost of system equipment.

equipment. The absorption chiller has the highest initial investment cost among all the system equipment (29%), accounting for almost one-third of the total investment cost. This is because a higher unit heat cost results in a higher capital investment cost of the absorption chiller, which can also be reflected in the PEM electrolyzer. The unit cost of the PEM electrolyzer is 1000 \$/kW, as depicted in Table 3, and the initial investment cost of the PEM electrolyzer accounts for 16% of the total investment cost. To improve the performance of the gas turbine cycle, a large amount of air is needed for combustion between mixture gas (biogas, natural gas) and oxygen. Hence the size of the air compressor and gas turbine increases and the initial investment of these components increase accordingly. The ratio of the air compressor and gas turbine are 18% and 10%, respectively. Moreover, the initial investment cost of the geothermal well is about 15%, this is mainly due to high borehole cost, such as drilling task, construction and material expense.

5.3.3. Comparison of unit exergy cost of products between two different methods

Fig. 9 shows the variations in the unit exergy cost of products for two different methods. The modified method has a higher unit exergy cost of electricity and hydrogen than that of the conventional exergoeconomic method. The unit exergy cost of hot water and chilled water under the modified method are lower than that under conventional method. The cost rate of electricity and hydrogen all increase, while the cost rate of hot water and chilled water all decrease in different degrees, considering the energy level in the auxiliary cost equation. These phenomena are in accordance with the principle of good quality and high price. In addition, hot water (HX-02) has the highest unit exergy cost and electricity has the lowest in the conventional method, because of the following reasons: 1) As the exergy values of hot water and chilled water are lower than that of electricity and hydrogen, the unit exergy cost of the former is higher than that of the latter. 2) The hot water in HX-02 mainly absorbed the sensible heat of bio-gas, and the absorption chiller is driven by flue gas. The mass flow rate of flue gas is greater than that of bio-gas, and the exergy of chilled water is higher than that of hot water in HX-02, because of which the unit exergy cost of chilled water is lower than that of hot water (HX-02). 3) Water (stream 31) is heated by the condenser and HX. The utilization of the ground source heat pump increases the flow rate of hot water and the exergy output of hot water increases accordingly. In addition, the unit exergy cost of hot water in HX is relatively higher besides the unit exergy cost of hot water in HX-02. The reason for this is the high capital investment cost of ground source heat pump, especially the cost of the geothermal well. On the other hand, although the capital investment cost of absorption chiller is greater than that of ground source heat pump, the exergy of chilled water is higher than that of hot water (HX). Hence the unit exergy cost of hot water in HX is higher than that of chilled water. In addition to this, as the decreasing cost rate of hot water in HX-02 is higher than that of chilled water, the unit exergy cost of hot water (HX-02) is lower than that of chilled water in the modified method.

5.3.4. Sensitivity analysis

To further investigate the influences of some economic parameters (biomass and natural gas price, service life, interest rate and operating time coefficient) on unit exergy cost of products for conventional and modified exergoeconomic methods, sensitivity analysis is a suitable selection. The variations in unit exergy cost of products can be reflected clearly by increasing or decreasing these economic factors, which are shown in Figs. 10–14.

The influence of biomass cost on the unit exergy cost of products under two different exergoeconomic methods is illustrated in Fig. 10. The benchmark cost of biomass is 57.2 \$/ton and the floating range is −25% to +25%. (Because there are many issues affecting the biomass price: characteristics (calorific value, ash or moisture content), processing technology, transportation distance, etc.; this section only considers the effect of biomass price itself on unit exergy cost of products.) As shown in the figure, the unit exergy cost of all products increases with an increase in biomass cost, and their growth rates are distinct not only for different exergoeconomic methods but also for different products. In the conventional exergoeconomic method, the unit exergy cost of hot water (HX-02) exhibits the highest growth rate of approximately 56.15%. This is considerably greater than the unit exergy cost of electricity by approximately 15.79%. The unit exergy cost of hot water (HX) has the lowest growth rate, which increases from 59.95 \$/GJ to 63.15 \$/GJ, an increase of 5.34%. Moreover, both the modified and conventional exergoeconomic methods have similar variations in product cost except the distinction of growth rate. The increasing range of the unit exergy costs of electricity and hydrogen under the modified method is higher than that under the conventional method, while the increasing range of the unit exergy cost of hot water (HX, HX-02) and chilled water under the modified method is slightly lower than that under the conventional method.

Fig. 11 presents the influence of natural gas on the unit exergy cost of products under two different exergoeconomic methods. Similarly, the variation range of natural gas price is set at −25% to +25% with a benchmark cost of 0.528 $\$/m^3$. The unit exergy cost of products increases with increasing natural gas cost except for the unit exergy cost of hot water (HX-02), which remains constant with variations in natural

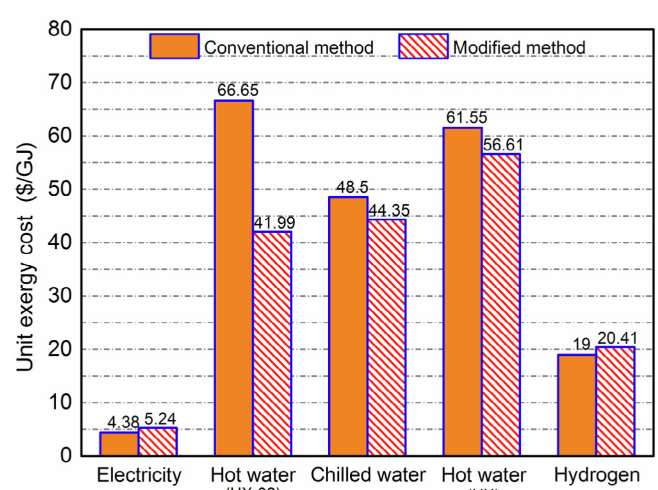

Fig. 9. Unit exergy cost of system products under two different methods.

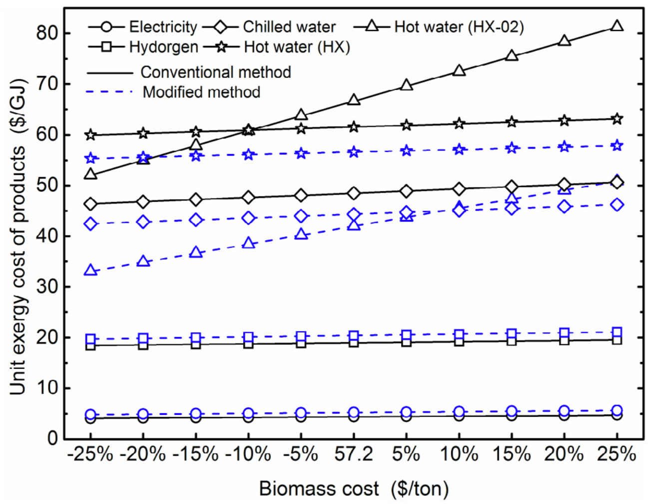

Fig. 10. Effect of biomass price on unit exergy cost of products.

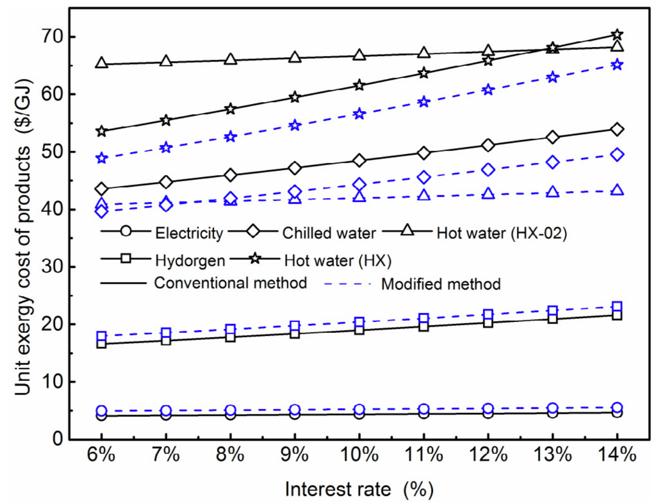

Fig. 13. Effect of interest rate on unit exergy cost of products.

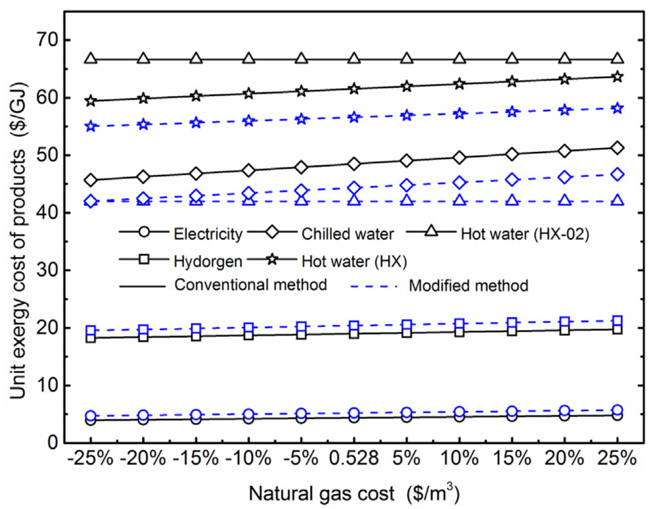

Fig. 11. Effect of natural gas price on unit exergy cost of products.

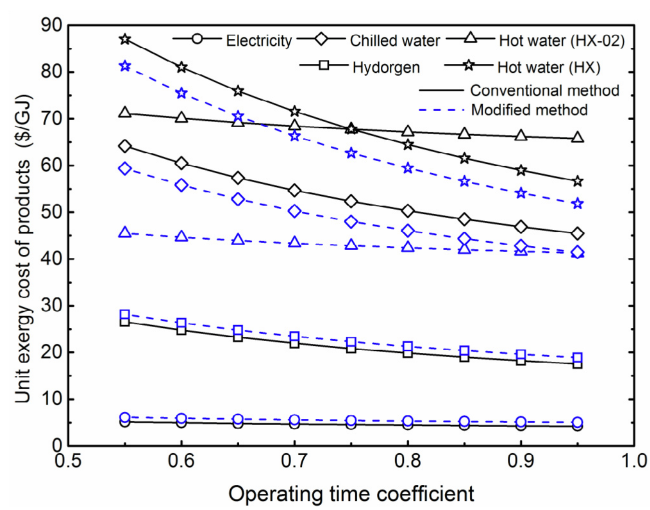

Fig. 14. Effect of operating hour on unit exergy cost of products.

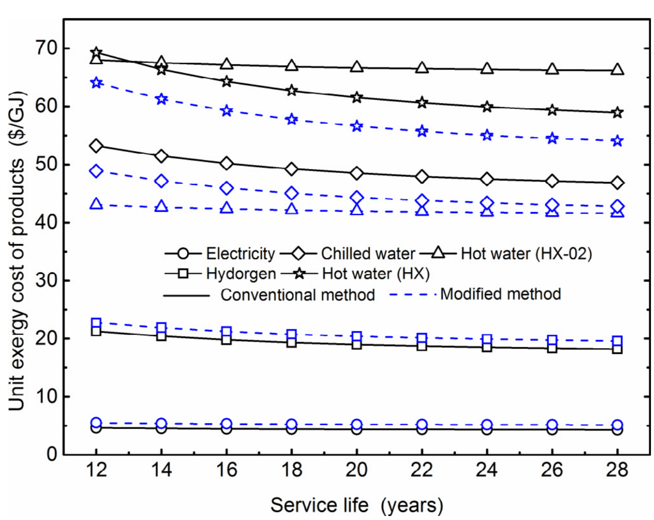

Fig. 12. Effect of service life on unit exergy cost of products.

gas. This can be explained by the fact that when the natural gas is mixed with bio-gas in gas mixer after biomass is gasified in gasifier, the output of hot water in HX-02 is not affected by natural gas but by the sensible heat of bio-gas from the gasifier, which is clearly illustrated in Fig. 1. Hence, the unit exergy cost of hot water (HX-02) does not vary with variations in natural gas cost. In conventional method, the unit exergy cost of products is similar to that of the modified method. In the conventional method, the highest growth rate occurs in the unit exergy cost of electricity, which is approximately 21.26%, followed by the unit exergy costs of hot water, chilled water and hydrogen at 7.08%, 12.25% and 7.93%, respectively.

The influence of service life on the unit exergy cost of products under two different exergoeconomic methods is shown in Fig. 12. The service life varies from 12 to 28 at the benchmark year of 20. In the figure, the unit exergy cost of products decreases non-linearly as service life increases, and the decreasing rate of these products vary. In the specified variation range, the unit exergy cost of hot water (HX) has the highest decreasing rates, which are 14.93% and 15.62% in conventional and modified methods, respectively. Therefore, the unit exergy cost of hot water (HX) is more sensitive to service life than others. In addition, the lowest decreasing rate belongs to hot water (HX-02) at 2.68% and 3.32% in conventional and modified methods, respectively.

Fig. 13 depicts the influence of interest rate on unit exergy cost of products under two different exergoeconomic methods; the interest rate varies from 6% to 14% at the benchmark interest rate of 10%. It can be seen from the figure that the unit exergy cost of products increases with increasing interest rate. The highest increasing rate is unit exergy cost of hot water (HX) in both conventional and modified methods, which are 31.35% and 33.31%, respectively. Moreover, the unit exergy cost of hot water (HX-02) is less sensitive to interest rate than others and their values are 4.52% and 5.65% in both conventional and modified methods, respectively.

The influence of operating time coefficient on the unit exergy cost of products is shown in Fig. 14, the operating time coefficient increases from 55% to 95% at the benchmark hour of 8760 h. In the picture, the unit exergy cost of products decreases non-linearly as operating time coefficient increases. In the conventional method, the decreasing rates of the unit exergy cost of electricity, hot water (HX-02), chilled water, hot water (HX), and hydrogen are 17.87%, 7.51%, 29.17%, 34.92% and 33.96%, respectively; and the decreasing rates of unit exergy cost of electricity, hot water (HX-02), chilled water, hot water (HX) and hydrogen in the modified method are 17.35%, 9.19%, 30.17%, 36.23% and 32.87%, respectively. Therefore, the unit exergy cost of hot water (HX) is most sensitive to operating time coefficient, and that of hot water (HX-02) is the least sensitive.

6. Conclusion

In the present work, a novel polygeneration system based on biomass gasification, gas turbine cycle, ground source heat pump and PEM electrolyzer is proposed. Energy level based cost allocation method is adopted in the modified exergoeconomic analysis, and exergoeconomic performances of the proposed system are compared under conventional and modified methods. Moreover, the exergy analysis of proposed system is also investigated. Main conclusions of this study can be summarized as:

(1) With increasing current density, the energy and exergy of PEM electrolyzer first decreases sharply at a low current density, and then decreases slowly at a high current density. For the electrolyzer, the energy efficiency is a little higher than the exergy efficiency. In the practical utilization process, it is necessary to select a suitable current density that contributes towards obtaining optimum hydrogen levels and a more efficient electrolysis process. In addition, the energy and exergy efficiencies of the proposed system decrease with the increase in the current density of the electrolyzer, which is in accord with the variable efficiencies in electrolyzer.

(2) In the exergy analysis, the highest exergy destruction occurs in the combustor, followed by the absorption chiller and gasifier. On the one hand the main inputs (bio-gas and natural gas) are utilized in the combustor; while on the other hand, the irreversibility of the combustion process is dominant. All these factors result in the highest exergy destruction of the combustor. Moreover, the exergy efficiency of HX-02, HX and absorption chiller is relatively lower than others considering the low exergy value of the outputs (hot water and chilled water).

(3) A comparative analysis of exergoeconomic performances is conducted. Considering the effect of the energy level, the unit exergy cost of products under modified exergoeconomic method is more reasonable than that of products under conventional exergoeconomic method. In the energy level based exergoeconomic method, the unit exergy cost of electricity, hot water (HX-02), chilled water, hot water (HX) and hydrogen is 5.24 $/GJ, 41.99 $/GJ, 44.35 $/GJ, 56.61 $/GJ and 20.41 $/GJ, respectively; and the unit exergy cost of electricity, hot water (HX-02), chilled water, hot water (HX) and hydrogen is 4.38 $/GJ, 66.65 $/GJ, 48.50 $/GJ, 61.55 $/GJ and 19.00 $/GJ under the conventional exergoeconomic method. The unit exergy cost of electricity and hydrogen under energy level based exergoeconomic method is higher than that under the conventional exergoeconomic method, while the unit exergy cost of hot water and chilled water under the energy level based exergoeconomic method is lower than that under the conventional exergoeconomic method. Furthermore, the exergoeconomic factor and relative cost difference of system equipment also show distinctions under conventional and energy level based exergoeconomic methods. The exergoeconomic factors of the gasifier, HX-01, HX-02. HX-03, absorption chiller, and HX under the modified method are a little higher than that under conventional method, and the exergoeconomic factors of other equipment show the opposite trend. Finally, the sensitivity analysis of the unit exergy cost of products (electricity, hot water, chilled water and hydrogen) is investigated and a comparison of unit cost variation under two different exergoeconomic methods is also carried out.

The proposed polygeneration system integrates with renewable energy (such as biomass and geothermal energy) and fossil fuel (natural gas), which provides power, hot water, chilled water and hydrogen for users. On the one hand, the natural gas contributes to increase the stability of energy system; on the other hand, the conversion of electricity to hydrogen can improve the flexibility of energy system.

Declaration of Competing Interest

None.

Acknowledgements

This study is supported by the National Natural Science Foundation of China (NO.51806021, 51806022, 51706022), Key Laboratory of Efficient & Clean Energy Utilization, The Education Department of Hunan Province (2018NGQ005), Natural Science Foundation of Hunan Province (NO.2016JJ2021, 2018JJ3545), Scientific Research Fund of Hunan Provincial Education Department (NO. 18C0178, 16B001, 16B012) and State Key Laboratory of Air-conditioning Equipment and System Energy Conservation (NO. ACSKL2018KT18).

References

[1] IEA. Global energy and CO2 status report 2017. http://www.iea.org/statistics/.
[2] IEA. Renewable information: overview 2018. http://www.iea.org/statistics/.
[3] Sansaniwal SK, Rosen MA, Tyagi SK. Global challenges in the sustainable development of biomass gasification: an overview. Renew Sustain Energy Rev 2017;80:23–43. https://doi.org/10.1016/j.rser.2017.05.215.
[4] CNREC China. National Renewable Energy Center. China Renewable Energy Outlook; 2018.
[5] Bai Z, Liu T, Liu Q, et al. Performance investigation of a new cooling, heating and power system with methanol decomposition based chemical recuperation process. Appl Energy 2018;229:1152–63. https://doi.org/10.1016/j.apenergy.2018.07.112.
[6] Zhao P, Dai Y, Wang J. Performance assessment and optimization of a combined heat and power system based on compressed air energy storage system and humid air turbine cycle. Energy Convers Manage 2015;103:562–72. https://doi.org/10.1016/j.enconman.2015.07.004.
[7] Rostamzadeh H, Gargari SG, Namin AS, et al. A novel multigeneration system driven by a hybrid biogas-geothermal heat source, Part II: multi-criteria optimization. Energy Convers Manage 2019;180:859–88. https://doi.org/10.1016/j.enconman.2018.11.035.
[8] Habibollahzade A, Gholamian E, Houshfar E, et al. Multi-objective optimization of biomass-based solid oxide fuel cell integrated with Stirling engine and electrolyzer. Energy Convers Manage 2018;171:1116–33. https://doi.org/10.1016/j.enconman.2018.06.061.
[9] Liu Z, Liu Y, He BJ, et al. Application and suitability analysis of the key technologies in nearly zero energy buildings in China. Renew Sustain Energy Rev 2019;101:329–45. https://doi.org/10.1016/j.rser.2018.11.023.
[10] Ahmadi P, Dincer I, Rosen MA. Development and assessment of an integrated biomass-based multi-generation energy system. Energy 2013;56:155–66. https://doi.org/10.1016/j.energy.2013.04.024.
[11] Bai Z, Liu Q, Lei J, et al. New solar-biomass power generation system integrated a two-stage gasifier. Appl Energy 2017;194:310–9. https://doi.org/10.1016/j.apenergy.2016.06.081.
[12] Mohammadi A, Mehrpooya M. Energy and exergy analyses of a combined desalination and CCHP system driven by geothermal energy. Appl Therm Eng 2017;116:685–94. https://doi.org/10.1016/j.applthermaleng.2017.01.114.
[13] Amirmohammad B, Ehsan G, Pouria A, et al. Energy, exergy and exergoeconomic (3E) analyses and multi-objective optimization of a solar and geothermal based integrated energy system. Appl Therm Eng 2018;143:1011–22. https://doi.org/10.1016/j.applthermaleng.2018.08.034.
[14] He WF, Han D, Wen T. Energy, entropy and cost analysis of a combined power and water system with cascade utilization of geothermal energy. Energy Convers

Manage 2018;174:719–29. https://doi.org/10.1016/j.enconman.2018.08.089.
[15] Malik M, Dincer I, Rosen MA. Development and analysis of a new renewable energy-based multi-generation system. Energy 2015;79:90–9. https://doi.org/10.1016/j.energy.2014.10.057.
[16] Srinivas S, Eisenberg D, Seifkar N, et al. Simulation-based study of a novel integration: geothermal-biomass power plant. Energy Fuels 2014;28(12):7632–42. https://doi.org/10.1021/ef501601b.
[17] Segurado R, Pereira S, Correia D, et al. Techno-economic analysis of a trigeneration system based on biomass gasification. Renew Sustain Energy Rev 2019;103:501–14. https://doi.org/10.1016/j.rser.2019.01.008.
[18] Zhang X, Li H, Liu L, et al. Exergetic and exergoeconomic assessment of a novel CHP system integrating biomass partial gasification with ground source heat pump. Energy Convers Manage 2018;156:666–79. https://doi.org/10.1016/j.enconman.2017.11.075.
[19] Zhang X, Li H, Liu L, et al. Optimization analysis of a novel combined heating and power system based on biomass partial gasification and ground source heat pump. Energy Convers Manage 2018;163:355–70. https://doi.org/10.1016/j.enconman.2018.02.073.
[20] Zhang X, Liu X, Sun X, et al. Thermodynamic and economic assessment of a novel CCHP integrated system taking biomass, natural gas and geothermal energy as co-feeds. Energy Convers Manage 2018;172:105–18. https://doi.org/10.1016/j.enconman.2018.07.002.
[21] Zhang H, Lin G, Chen J. Evaluation and calculation on the efficiency of a water electrolysis system for hydrogen production. Int J Hydrogen Energy 2010;35(20):10851–8. https://doi.org/10.1016/j.ijhydene.2010.07.088.
[22] Ahmadi P, Dincer I, Rosen MA. Energy and exergy analyses of hydrogen production via solar-boosted ocean thermal energy conversion and PEM electrolysis. Int J Hydrogen Energy 2013;38(4):1795–805. https://doi.org/10.1016/j.ijhydene.2012.11.025.
[23] Mohammadi A, Mehrpooya M. A comprehensive review on coupling different types of electrolyzer to renewable energy sources. Energy 2018;158:632–55. https://doi.org/10.1016/j.energy.2018.06.073.
[24] Kianfard H, Khalilarya S, Jafarmadar S. Exergy and exergoeconomic evaluation of hydrogen and distilled water production via combination of PEM electrolyzer, RO desalination unit and geothermal driven dual fluid ORC. Energy Convers Manage 2018;177:339–49. https://doi.org/10.1016/j.enconman.2018.09.057.
[25] Behzadi A, Habibollahzade A, Ahmadi P, et al. Multi-objective design optimization of a solar based system for electricity, cooling, and hydrogen production. Energy 2019;169:696–709. https://doi.org/10.1016/j.energy.2018.12.047.
[26] Moharamian A, Soltani S, Rosen MA, et al. Advanced exergy and advanced exergoeconomic analyses of biomass and natural gas fired combined cycles with hydrogen production. Appl Therm Eng 2018;134:1–11. https://doi.org/10.1016/j.applthermaleng.2018.01.103.
[27] Gholamian E, Habibollahzade A, Zare V. Development and multi-objective optimization of geothermal-based organic Rankine cycle integrated with thermoelectric generator and proton exchange membrane electrolyzer for power and hydrogen production. Energy Convers Manage 2018;174:112–25. https://doi.org/10.1016/j.enconman.2018.08.027.
[28] Taheri MH, Mosaffa AH, Farshi LG. Energy, exergy and economic assessments of a novel integrated biomass based multigeneration energy system with hydrogen production and LNG regasification cycle. Energy 2017;125:162–77. https://doi.org/10.1016/j.energy.2017.02.124.
[29] Siddiqui O, Dincer I. Examination of a new solar-based integrated system for desalination, electricity generation and hydrogen production. Sol Energy 2018;163:224–34. https://doi.org/10.1016/j.solener.2018.01.077.
[30] Bejan A, Tsatsaronis G, Moran M. Thermal design and optimization. New York: John Wiley & Sons; 1996.
[31] Abusoglu A, Kanoglu M. Exergoeconomic analysis and optimization of combined heat and power production: a review. Renew Sustain Energy Rev 2009;13(9):2295–308. https://doi.org/10.1016/j.rser.2009.05.004.
[32] Ghaebi H, Farhang B, Parikhani T, et al. Energy, exergy and exergoeconomic analysis of a cogeneration system for power and hydrogen production purpose based on TRR method and using low grade geothermal source. Geothermics 2018;71:132–45. https://doi.org/10.1016/j.geothermics.2017.08.011.
[33] Baghernejad A, Yaghoubi M, Jafarpur K. Exergoeconomic comparison of three novel trigeneration systems using SOFC, biomass and solar energies. Appl Therm Eng 2016;104:534–55. https://doi.org/10.1016/j.applthermaleng.2016.05.032.
[34] Anvari S, Khoshbakhti Saray R, Bahlouli K. Conventional and advanced exergetic and exergoeconomic analyses applied to a tri-generation cycle for heat, cold and power production. Energy 2015;91:925–39. https://doi.org/10.1016/j.energy.2015.08.108.
[35] Qi H, Han W, Zhang N. Exergy cost allocation method based on energy level and its application. J Eng Therm 2016;37(6):1141–6.
[36] Qi H, Han W, Zhang N, et al. Exergoeconomic analysis methodology based on energy level and case study. Proc CSEE 2016;36(12):3223–30.
[37] Wang Z, Han W, Zhang N, et al. Exergy cost allocation method based on energy level (ECAEL) for a CCHP system. Energy 2017;134:240–7. https://doi.org/10.1016/j.energy.2017.06.015.
[38] Ning J, Guo P, Tang X. The energy quality factor method and its application in determining economic cost of product's unit exergy flow in multiple co-generation system. Therm Power Gener 2010;39(2):41–5.
[39] Zhou J, Qin Y, Sun Z. Analysis of algebraic mode for thermal economics in distributed energy stations. Therm Power Gener 2007;6:29–32.
[40] Ishida M. Thermodynamics made comprehensible. Nova Science Pub Incorporated; 2002.
[41] Wang Z, Han W, Zhang N, et al. Energy level difference graphic analysis method of combined cooling, heating and power systems. Energy 2018;160:1069–77. https://doi.org/10.1016/j.energy.2018.07.026.
[42] Chen Q, Han W, Zheng JJ, et al. The exergy and energy level analysis of a combined cooling, heating and power system driven by a small scale gas turbine at off design condition. Appl Therm Eng 2014;66(1–2):590–602. https://doi.org/10.1016/j.applthermaleng.2014.02.066.
[43] Gao P, Dai Y, Tong YW, et al. Energy matching and optimization analysis of waste to energy CCHP (combined cooling, heating and power) system with exergy and energy level. Energy 2015;79:522–35. https://doi.org/10.1016/j.energy.2014.11.050.
[44] Wang Z, Han W, Zhang N, et al. Assessment of off-design performance of a combined cooling, heating and power system using exergoeconomic analysis. Energy Convers Manage 2018;171:188–95. https://doi.org/10.1016/j.enconman.2018.05.055.
[45] Wang J, Mao T, Wu J. Modified exergoeconomic modeling and analysis of combined cooling heating and power system integrated with biomass-steam gasification. Energy 2017;139:871–82. https://doi.org/10.1016/j.energy.2017.08.030.
[46] Wang J, Li M, Ren F, et al. Modified exergoeconomic analysis method based on energy level with reliability consideration: cost allocations in a biomass trigeneration system. Renew Energy 2018;123:104–16. https://doi.org/10.1016/j.renene.2018.02.040.
[47] Zhang X, Li H, Liu L, et al. Thermodynamic and economic analysis of biomass partial gasification process. Appl Therm Eng 2018;129:410–20. https://doi.org/10.1016/j.applthermaleng.2017.10.069.
[48] Ahmadi P, Dincer I, Rosen MA. Performance assessment and optimization of a novel integrated multigeneration system for residential buildings. Energy Build 2013;67(6):568–78. https://doi.org/10.1016/j.enbuild.2013.08.046.
[49] Ni M, Leung MKH, Leung DYC. Energy and exergy analysis of hydrogen production by a proton exchange membrane (PEM) electrolyzer plant. Energy Convers Manage 2008;49(10):2748–56. https://doi.org/10.1016/j.enconman.2008.03.018.
[50] Puig-Arnavat M, Bruno JC, Coronas A. Review and analysis of biomass gasification models. Renew Sustain Energy Rev 2010;14(9):2841–51. https://doi.org/10.1016/j.rser.2010.07.030.
[51] Habibollahzade A, Gholamian E, Ahmadi P, et al. Multi-criteria optimization of an integrated energy system with thermoelectric generator, parabolic trough solar collector and electrolysis for hydrogen production. Int J Hydrogen Energy 2018;43(31):14140–57. https://doi.org/10.1016/j.ijhydene.2018.05.143.
[52] Tijani AS, Rahim AA. Numerical modeling the effect of operating variables on Faraday efficiency in PEM electrolyzer. Proced Tech 2016;26:419–27. https://doi.org/10.1016/j.protcy.2016.08.054.
[53] Tijani AS, Binti Kamarudin NA, Binti Mazlan FA. Investigation of the effect of charge transfer coefficient (CTC) on the operating voltage of polymer electrolyte membrane (PEM) electrolyzer. Int J Hydrogen Energy 2018;43(19):9119–32. https://doi.org/10.1016/j.ijhydene.2018.03.111.
[54] El-Emam RS, Dincer I. Development and assessment of a novel solar heliostat-based multigeneration system. Int J Hydrogen Energy 2018;43(5):2610–20. https://doi.org/10.1016/j.ijhydene.2017.12.026.
[55] Nieminen J, Dincer I, Naterer G. Comparative performance analysis of PEM and solid oxide steam electrolysers. Int J Hydrogen Energy 2010;35(20):10842–50. https://doi.org/10.1016/j.ijhydene.2010.06.005.
[56] Lazzaretto A, Tsatsaronis G. SPECO: a systematic and general methodology for calculating efficiencies and costs in thermal systems. Energy 2006;31(8):1257–89. https://doi.org/10.1016/j.energy.2005.03.011.
[57] Yang K, Zhu N, Ding Y, et al. Thermoeconomic analysis of an integrated combined cooling, heating and power system with biomass gasification. Energy Convers Manage 2018;171:671–82. https://doi.org/10.1016/j.enconman.2018.05.089.
[58] Ahmadi P, Dincer I. Thermodynamic analysis and thermoeconomic optimization of a dual pressure combined cycle power plant with a supplementary firing unit. Energy Convers Manage 2011;52(5):2296–308. https://doi.org/10.1016/j.enconman.2010.12.023.
[59] Habibollahzade A, Gholamian E, Ahmadi P, et al. Exergoeconomic assessment and multi-objective optimization of a solar chimney integrated with waste-to-energy. Sol Energy 2018;176:30–41. https://doi.org/10.1016/j.solener.2018.10.016.
[60] Khanmohammadi S, Heidarnejad P, Javani N, et al. Exergoeconomic analysis and multi objective optimization of a solar based integrated energy system for hydrogen production. Int J Hydrogen Energy 2017;42(33):21443–53. https://doi.org/10.1016/j.ijhydene.2017.02.105.
[61] Zhang X, Zeng R, Mu K, et al. Exergetic and exergoeconomic evaluation of co-firing biomass gas with natural gas in CCHP system integrated with ground source heat pump. Energy Convers Manage 2019;180:622–40. https://doi.org/10.1016/j.enconman.2018.11.009.
[62] Huang J. Design and economical analysis of ground source heat pump for regional buildings. Build Energy Environ 2017;36(6):73–5.
[63] Jiang XZ, Wang X, Feng L, et al. Adapted computational method of energy level and energy quality evolution for combined cooling, heating and power systems with energy storage units. Energy 2017;120:209–16. https://doi.org/10.1016/j.energy.2016.12.124.
[64] Ahmadi MH, Mehrpooya M, Pourfayaz F. Exergoeconomic analysis and multi objective optimization of performance of a Carbon dioxide power cycle driven by geothermal energy with liquefied natural gas as its heat sink. Energy Convers Manage 2016;119:422–34. https://doi.org/10.1016/j.enconman.2016.04.062.
[65] Ioroi T, Yasuda K, Siroma Z, et al. Thin film electrocatalyst layer for unitized regenerative polymer electrolyte fuel cells. J Power Sources 2002;112(2):583–7. https://doi.org/10.1016/S0378-7753(02)00466-4.